ELSEVIER

Marine and Petroleum Geology 16 (1999) 1–25

Marine and Petroleum Geology

The Argentine continental margin north of 48°S: sedimentary successions, volcanic activity during breakup

K. Hinz, S. Neben*, B. Schreckenberger, H. A. Roeser, M. Block, K. Goncalves de Souza, H. Meyer

Bundesanstalt für Geowissenschaften und Rohstoffe, P.O. Box 51 01 53, 30631 Hannover, Germany

Received 15 May 1998; revised 23 July 1998; accepted 27 July 1998

Abstract

New seismic data and geophysical results from the outer Argentine continental margin and from seismic flow-line transects across the oceanic Argentine/Brazil and Cape/Angola Basins are presented. The results document that the Early Cretaceous South Atlantic continental breakup and initial sea-floor spreading were accompanied by large-scale, transient volcanism emplacing voluminous extrusive constructions on the conjugate outer continental margins of the South Atlantic. On the Argentine margin we interpret three major tectono-volcanic crustal units beneath a thick and tectonically undisturbed sedimentary succession of Cretaceous and Tertiary age: (1) Syn-rift basins and even pre-rift features are present on the outer shelf; (2) a deeply buried, 60–120 km wide and several thousand metres thick volcanic wedge occupies most of the slope. The wedge is characterized by seaward-dipping reflectors and is associated with the distinct magnetic Anomaly G; (3) the seaward adjacent oceanic crust of Cretaceous age shows isochronous changes of the seismic images along our flow-line transects, suggesting some form of episodicity of rich magma and poor to moderate magma supply at the pre-existing mid-ocean ridge of the South Atlantic during Cretaceous time.

Keywords: Volcanic passive margin; Argentine continental margin; Sedimentary succession; Variability of oceanic crust

1. Introduction and regional setting

The area under discussion comprises the outermost shelf, slope and rise of the over 1500 km long eastern Argentine continental margin, extending from the mouth of the Rio de la Plata at about 35°30′S in the north to the Falkland–Agulhas Plateau Fracture Zone at about 48°S in the south (Fig. 1). The area of investigation also encompasses the westernmost part of the deep-sea Argentine Basin.

The Argentine offshore area between 35°30′S and 48°S down to the 5000 m isobath of the Argentine Basin comprises approximately 570,000 km^2 of continental shelf which is about 150–500 km wide, and approximately 450,000 km^2 of the slope and rise with water depths between 200 and 5000 m.

A complex set of sedimentary basins exist in the Argentine coastal and inner shelf area. These basins are from north to south (Fig. 9): Salado, Colorado, Rawson–Valdes, San Jorge and North Malvinas, following the trend of Paleozoic or Precambrian basement fabrics. The geology of these basins which originated during a major Late Jurassic through Early Cretaceous rift event has been discussed in publications by Uliana, Biddle and Cerdan (1989), Stoakes, Campbell, Cass and Ucha (1991), Fitzgerald, Mitchum, Uliana and Biddle (1990), Keeley and Light (1993), Ramos and Turic (1996).

Our geophysical surveys are focussed on the outer part of the Argentine continental margin where studies of magnetic and gravimetric data (LaBrecque & Rabinowitz, 1977; Rabinowitz & LaBrecque, 1979) infer the boundary between continental and oceanic crust to occur. The scientific objective of our geophysical studies was to search the Argentine continental margin for evidence of a remarkable continent-ocean boundary structure previously observed on the conjugate margin of southwest Africa (Hinz, 1981; Austin & Uchupi, 1982; Gerrard & Smith, 1983; Sibuet et al., 1984).

In this article we present the results of our geophysical studies, we describe events during crustal breakup and the early opening of the South Atlantic, and we report on isochronous changes of the seismic images of the Cretaceous-aged oceanic crust of the South Atlantic.

* Corresponding author. Tel.: 0049-511-643 3128; fax: 0049-511-643 3623; e-mail: neben@sdac.hannover.bgr.de

S0264–8172/99/$ - see front matter
PII: S0264–8172(98)00060–9

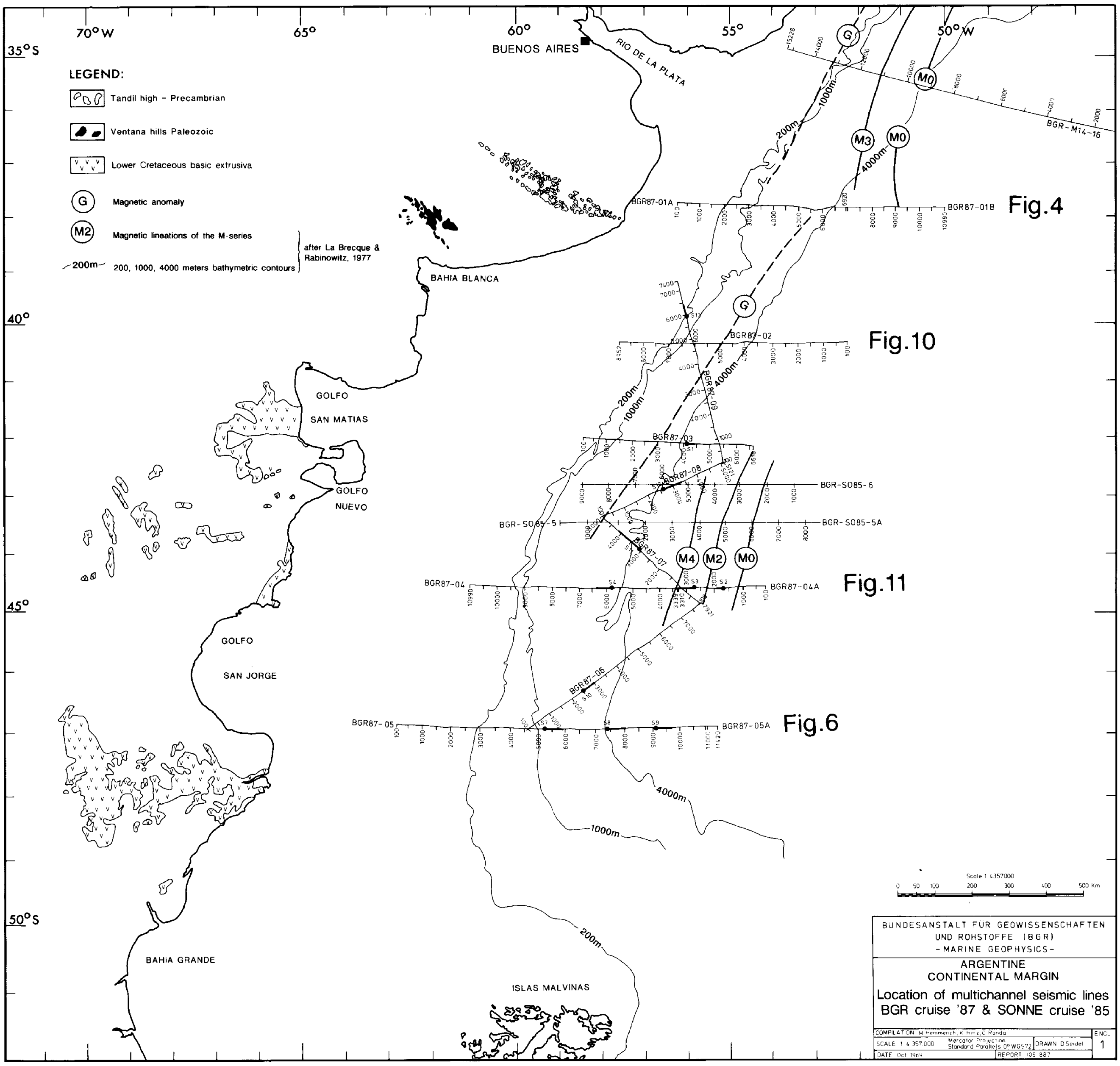

Fig. 1. Location of multichannel seismic reflection lines of BGR cruise 1987 and R/V SONNE cruise SO-85 1993.

2. Data acquisition and seismic processing

The BGR acquired 7931 km MCS lines in the Argentine Basin and on the outer Argentine continental margin during two cruises.

In 1987–1988 a total of 3676 km of multichannel seismic (MCS) lines (Fig. 1) with a coverage of 3000% were recorded together with gravity measurements using former Prakla-Seismos A.G.'s vessel S.V. EXPLORA. The vessel was equipped with a Sercel SN 358 DMX digital seismic recording system, a 3000 m long, 60-trace streamer, and a tuned airgun array with 32 guns having a total volume of 80.4 l (4906 in^3). The operating pressure was 140 bar (2000 psi).

In 1993 the BGR surveyed 4255 km of 48-channel reflection, magnetic and gravity profiles in the western South Atlantic during R.V. SONNE cruise SO-85. Cruise SO-85 was designed to study the variability of the Argentine Basin oceanic crust along flow-line profiles over Early Tertiary–Early Cretaceous crust. This survey, which was hampered by very bad weather, also includes two lines with a total length of 942 km across the outer continental margin (Fritsch et al., 1993). The seismic equipment consisted of a Texas Instruments DFS V digital seismic recording system, a 48-trace streamer with an active length of 2400 m (Model AMG 37-43) and two tuned airgun arrays with 20 guns having a total volume of 51.2 l (3124 in^3).

The 1987–1988 seismic data were processed using conventional processing routines with velocity analyses every 3 km. After predictive deconvolution, multiple attenuation and dynamic corrections the traces of the CDP-gathers were stacked. The stacked CDP-traces were band-pass filtered and normalized. Only selected parts of the profiles were migrated.

For processing of the SO-85 MCS data the DISCO software was used. The determination of processing parameters and computation of stacking velocities were made with the interactive FOCUS system. Deconvolution processing before and after stack and f–k migration were applied.

3. Regional seismic unconformities

Due to scarcity of published data from industrial drilling on the outer shelf and missing seismic tie-lines to both the DSDP Site 358 (located in the northeastern Argentine Basin at 37°39.31′S, 35°57.82′W, WD 4990 m, TD 5832 m) and exploration wells there is much uncertainty about the age and nature of seismic unconformities and markers recognized in our seismic data. Nonetheless, by comparing our MCS data with both previous seismic interpretations from the Argentine Basin (Ewing, Ludwig & Ewing, 1964; Supko & Perch-Nielsen, 1977), and with the conjugate southwestern African continental margin (Austin & Uchupi, 1982; Gerrard & Smith, 1983), we have defined five regional seismic marker horizons:

A rift-phase unconformity, correlated with the major Late Jurassic through Early Cretaceous rift event, is difficult to define. The base of inferred syn-rift basins resting on a reflective (?)Paleozoic unit recognized locally beneath the outer shelf between 39°S and 41°S (Figs 2 and 3) might represent this crustal stretching episode.

Unconformity AR 1, the most prominent and extensive horizon, forms both the upper boundary of a reflective sequence, only locally observed beneath the outer shelf, and the top of buried, wedge-shaped bodies characterized by divergent and seaward-dipping reflectors (SDRS) underlying the slope (Figs 4 and 5). Ocean Drilling Program (ODP) results on the North Atlantic volcanic margins (Eldholm et al., 1987) are consistent with previous interpretations that these wedges consist of basaltic flows and volcani-clastic rocks extruded near or above sea-level immediate prior to and during the first stage of the opening. We interpret both the flat reflective sequence, only recognized locally beneath the outer shelf (Fig. 2), as well as the distinct wedge-shaped units underlying the present slope (Fig. 5) as equivalents of the Paraná flood basalts.

The reported ages of the Paraná flood basalts span the period of about 135–120 Ma (Amaral, Cordani, Kawashita & Reynolds, 1966; Sartori, Maciel Filho & Menegott, 1975; Cordiani, Sartori & Kawashita, 1980), but the bulk of the Paraná flood basalts is thought to be emplaced at about 133 Ma (Renne, Mertz, Teixeiva, Ens & Richards, 1993). We assume as a minimum age Hauterivian, about 125 Ma, (Kent and Gradstein (1986) time scale) for the unconformitiy AR 1 which occurs as a distinct erosional surface along the entire Argentine outer shelf between 41°S and 48°S, truncating basement and predicted syn-rift and older pre-rift units (Figs 2 and 8–12). It might well be that unconformity AR 1 is diachronous across the margin, becoming older westward towards the outer shelf.

Horizon AR 2 is interpreted to represent the top of an early-drift succession which was recognized above the inferred volcanic wedge of seaward-dipping reflectors and extending eastwards above the seaward adjacent oceanic crust of the older end of the Cretaceous Magnetic Quiet Zone (CMQZ). We consider the AR 2 horizon to be an equivalent of horizon A II in the conjugate eastern deep Cape Basin (Emery, Uchupi, Bowin, Phillips & Simpson, 1975), that was dated by DSDP wells 361 and 363 as Late Aptian (Bolli et al., 1978), probably representing the transition from euxinic to open oceanic conditions.

Horizon AR 3 forms the erosional surface of a drift sequence characterized by a sub-parallel pattern as well as by an aggradational and weakly-developed progradational pattern. The sequence occupies the entire area of the CMQZ of the Argentine Basin and presumably also the outer shelf north of 41°S.

For the sedimentary drift sequences below AR 3 in the Argentine basin, seismic interval velocities vary between 2.5 km^{-1} and 3 km^{-1}, whereas interval velocities on the outer shelf range between 4 km^{-1} and 4.6 km^{-1}. Piston cores on the flanks of the deep canyons that incise the continental slope show that the Late Cretaceous sediments are dominantly dark shales, while Early Tertiary sediments have high concentration of sandstones.

We infer an Early Campanian age (about 81 Ma, Kent & Gradstein (1986) time scale) for horizon AR 3 because our flow-line multichannel seismic data in the South Atlantic suggest an excessive episode of volcanism/magmatism along the central South Atlantic spreading ridge during Latest Cenomanian/Earliest Turonian through Early Campanian, i.e. about 90–81 Ma.

The sedimentary column of the Argentine slope and rise above horizon? AR 3 is characterized by a very complex reflection pattern including mound facies, giant dune-like features and numerous unconformities (Figs 6 and 7). This complex seismic pattern and especially the presence of giant sedimentary drifts (Hollister, Nowell & Jumars, 1984) suggest that deep water currents played an important role in the depositional regime in the Argentine Basin after the formation of the distinct horizon AR 3.

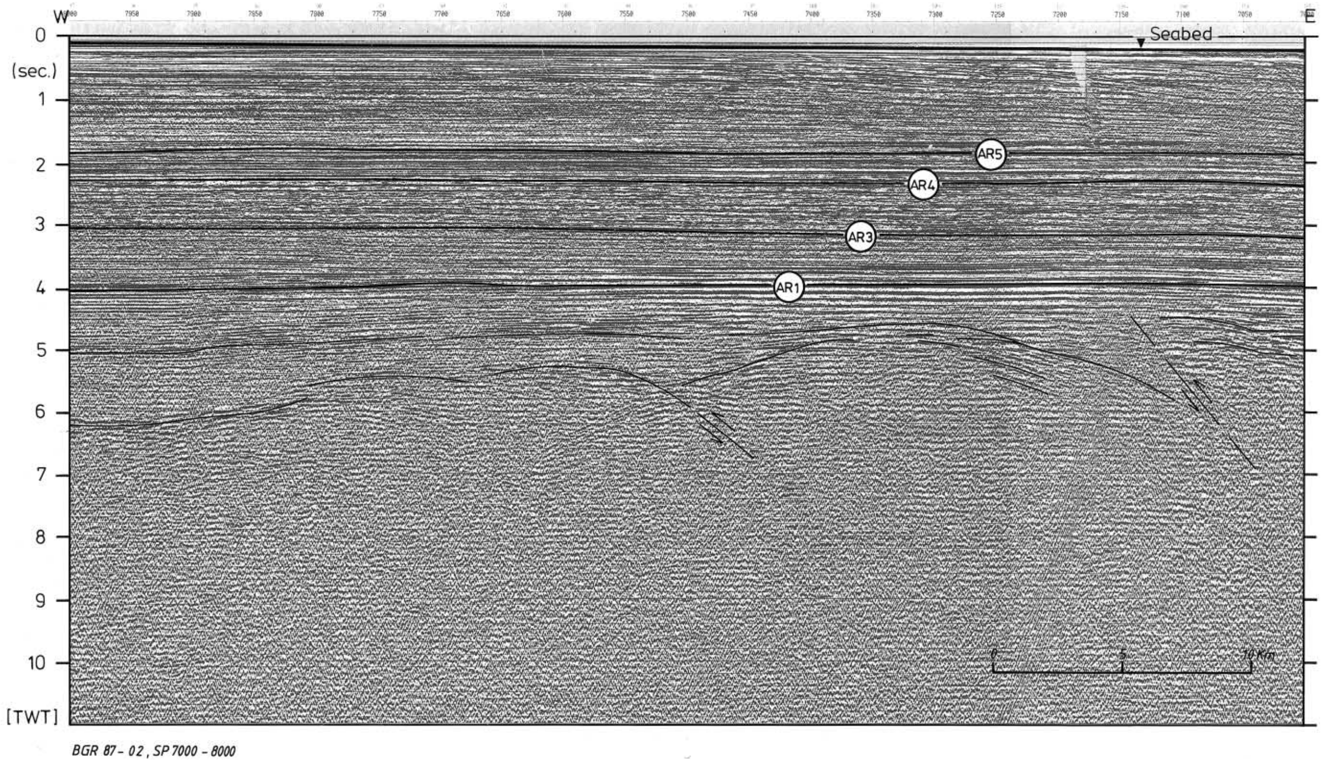

Fig. 2. Interpreted section of stacked multichannel reflection seismic profile BGR 87-02 showing a deeply buried syn-rift basin beneath unconformity AR1 described in the text. The syn-rift infill rests on a folded and faulted unit. Location on Fig. 10.

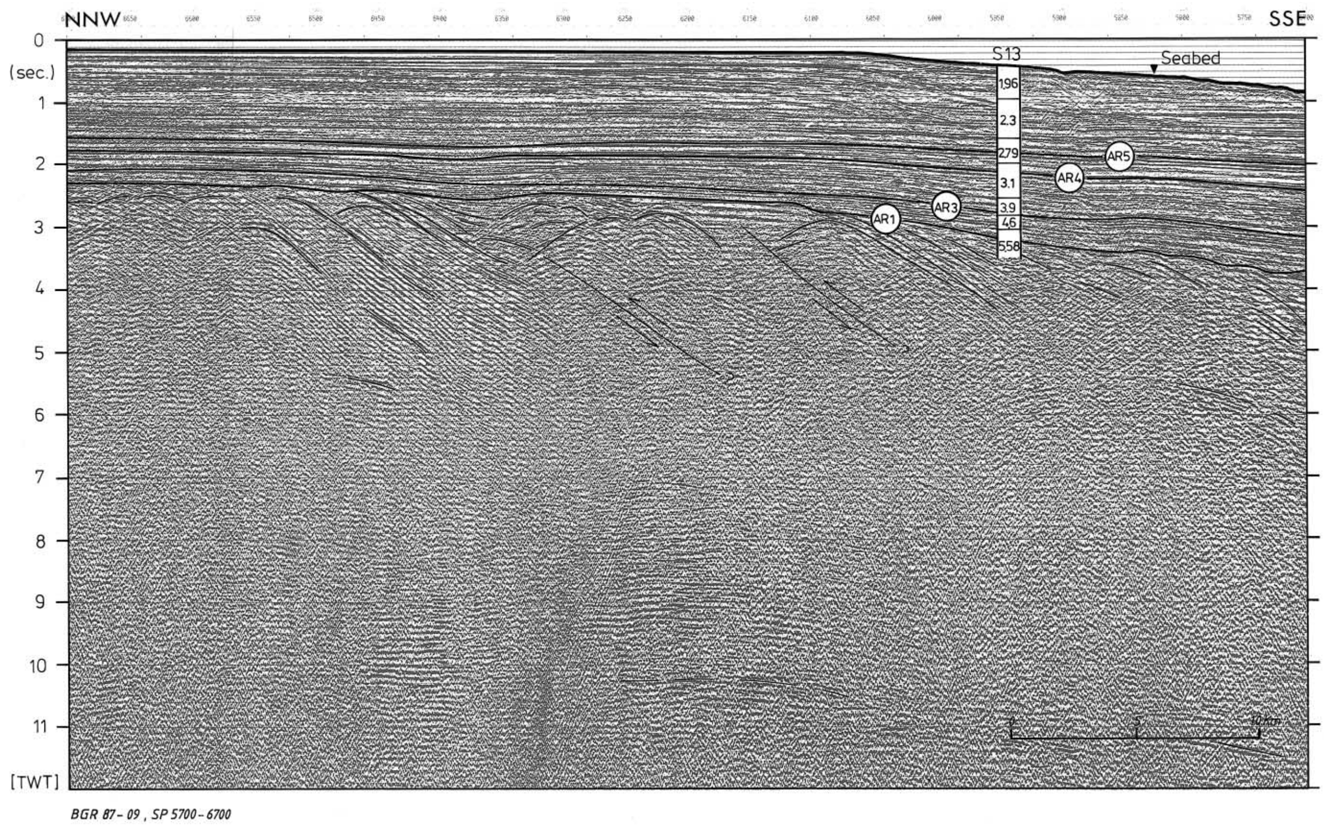

Fig. 3. Interpreted section of stacked multichannel seismic reflection profile BGR 87-09 showing asymmetrically folded Paleozoic deposits and inferred syn-rift troughs described in the text. S13 shows velocities (km^{-1}) of a sonobuoy refraction profile.

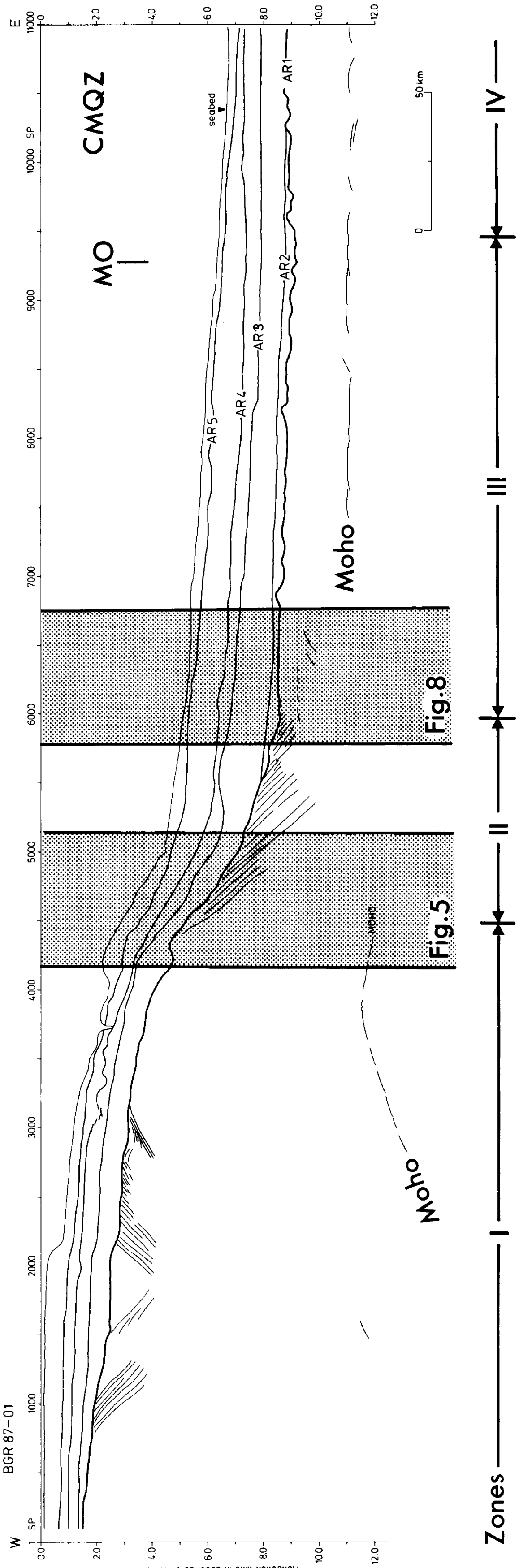

Fig. 4. Interpretation of reflection seismic line BGR 87-01 across the margin at 38°S. AR1–5 are regional unconformities. Defined structural zones I–IV are indicated. Location on Fig. 1.

Horizon AR 4 forms the base of a giant drift, 25–30 km wide and about 1200 m high (Fig. 7). ODP Leg 119 data from Prydz Bay, Antarctica (Barron et al., 1991; Cooper, Stagg & Geist, 1991) suggest initial major expansion of the grounded East Antarctic ice sheet toward the shelf edge occurred in the Late Eocene. This major East Antarctic ice expansion caused thermohaline circulation that affected the depositional regime in the Argentine Basin (Kennett & Shackleton, 1976; Supko & Perch-Nielsen, 1977). At DSDP Site 358, located in the northeastern Argentine Basin more than 1200 km from our survey area, a regional seismic reflection horizon named horizon B by Ewing and Lonardi (1971) correlates well with the current-controlled contact between Middle Eocene chalk and Late Eocene-Late Oligocene mudstone (Supko & Perch-Nielsen, 1977). Therefore, we assume a Late Eocene age for this horizon. The variable deep water current system during the Paleogene resulted in both the formation of giant drifts and mounds (Fig. 8) in some parts of the Argentine Basin, as well as in winnowing and bypassing in other parts.

Similarly, we tentatively attribute Horizon AR 5 to a renewed cooling and major expansion of the East Antarctic ice sheet including major cooling of the Antarctic Peninsula during the Middle Miocene (about 15 Ma, (Matthews & Poore, 1980; Kennett & Barker, 1990)).

4. Main structural units of the Argentine continental margin

Our seismic reconnaissance lines across the Argentine continental margin show a tectonically nearly undisturbed sedimentary succession of Cretaceous and Cenozoic age overlying a complex lower unit beneath the shelf and slope, and oceanic basement in the deep Argentine Basin (Figs 4, 6, 10 and 11). The structural elements of the lower rock unit, bounded at its top by unconformity AR 1, can be grouped into four regional structural zones shown in Fig. 9.

Zone I comprises the outer shelf and upper slope. Synrift basins and even pre-rift features have been observed in the seaward extension of the Salado and Colorado Basins beneath a sub-parallel bedded Mesozoic and Cenozoic succession with thicknesses in excess of 4 s, i.e. greater than 6000 m. The thickness of the predicted synrift basinal infill is in excess 1.5 s, i. e. greater than 2250 m (Figs 2 and 10). These deposits rest on a series of imbricate thrust sheets or asymmetrical folds characterized by high reflectivity and seismic velocities of more than 5 km^{-1} (Fig. 3). This imbricate unit follows the trend of the Ventana Hills and of the Precambrian Tandilia High. Permo-Carboniferous sedimentary rocks are exposed in the Ventana Hills consisting of an asymmetrical folded succession of diamictides, sandstones and dark shales more than 1500 m thick (Keeley & Light, 1993).

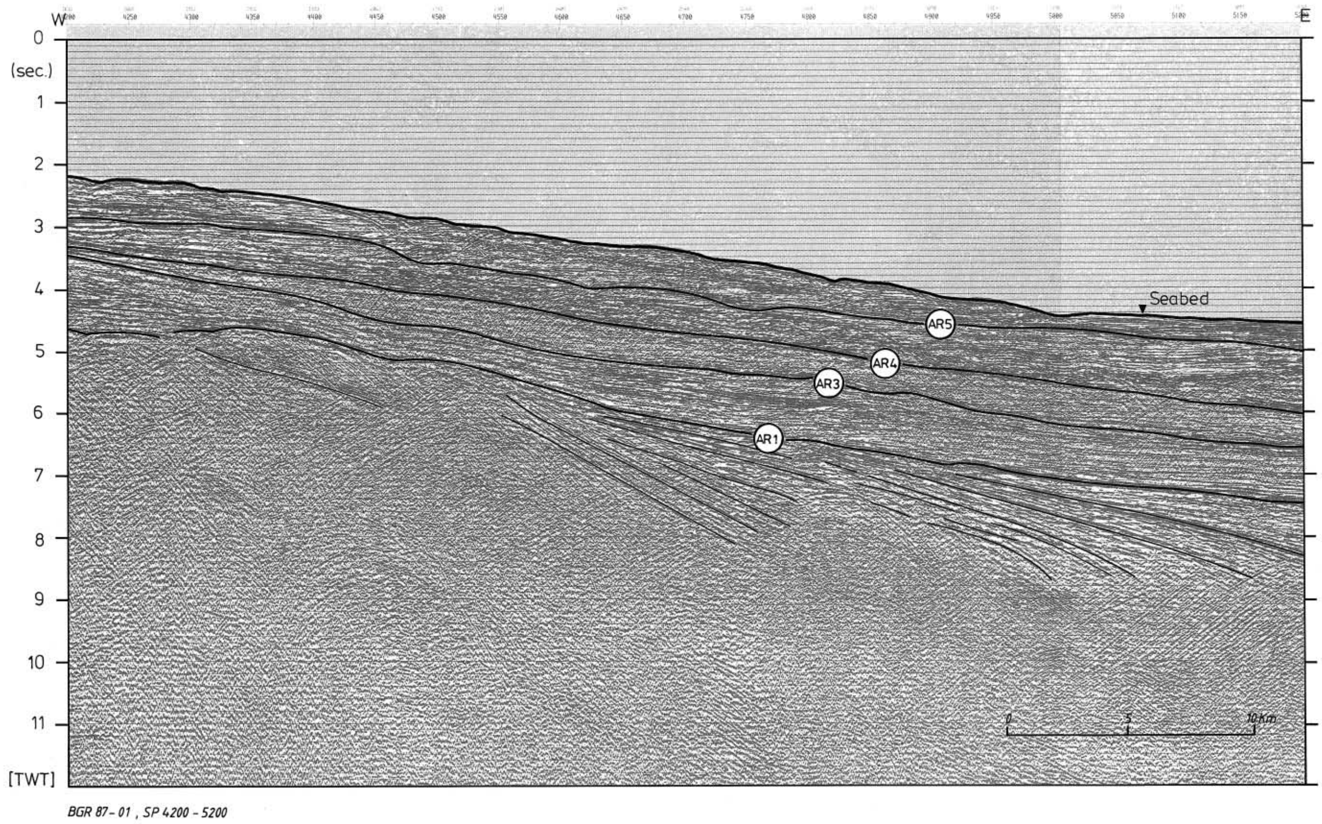

Fig. 5. Interpreted section of stacked multichannel reflection seismic profile BGR 87-01 showing a wedge-shaped body characterized by seaward-dipping reflectors described in the text. Location on Fig. 4.

Indications of the presence of syn-rift basins beneath the outer shelf between 41°S and 47°S are sparse. Here, peneplained basement of inferred Precambrian age is overlain by a sedimentary succession which is presumably younger than horizon AR 3 of inferred Campanian age. Some dipping reflections beneath the truncated surface of the basement suggest the presence of narrow half-grabens of unknown age and nature (Figs 11 and 12). There are some strong reflectors in deeper crustal levels. The occurrence of the recognized syn-rift and possibly pre-rift troughs, and the thickness (in reflection time) of their basinal infill is shown in Fig. 13.

Zone II occupies most of the slope and comprises the dominant structural feature of the Argentine continental margin that underlies a Mesozoic to Cenozoic sedimentary column. It is a 60–120 km wide wedge-shaped body characterized by an internally divergent pattern of reflections having ubiquitous seaward dip (Figs 5, 14 and 15). This remarkable deeply buried feature extends continuously from at least 48°S in the south to the continental margin of Uruguay, i.e. over a distance of more than 1200 km, and it continues northward to the region of the Campos Basin, offshore eastern Brazil (Goncalves de Souza, 1991).

Dips within the wedge are uniformly seaward and major individual reflections, which can be followed over distances from 10–20 km, are arcuate. The dip of individual reflections increases down-section from about 5–35°. The seismic velocities increase with depth from about 4 km^{-1} in the upper part to about 6 km^{-1} in the lower part of the body, yielding thicknesses in excess of 2.5–3.2 s, i.e. 5000–9600 m. Beneath the landward feather edge a basal termination is often recognizable (Fig. 3). Locally, some deep coherent reflection elements are present which might represent an antithetic block-faulted pre-rift substratum on which the wedge rests (Fig. 14).

The outer edge of the wedge is often characterized by short seaward-dipping reflections which terminate down-dip against an intra-crustal reflection between 9 and 10 s (Fig. 15). The inferred crust-mantle boundary deepens westwards with approaching the wedge (Fig. 15), and reaches depths of approximately 12 s (reflection time) beneath the feather edge (Fig. 14).

Zone II is more complex south of 43°S. The wedge consists of at least three wedge-shaped sequences which successively overlap, suggesting episodicity of emplacement (Fig. 16). The older sequence is characterized by a suite of seaward-dipping reflectors, whereas the younger and overlying sequences are characterized by a distinct smooth horizon constituting the top of each of these sequences with short seaward-dipping reflectors beneath.

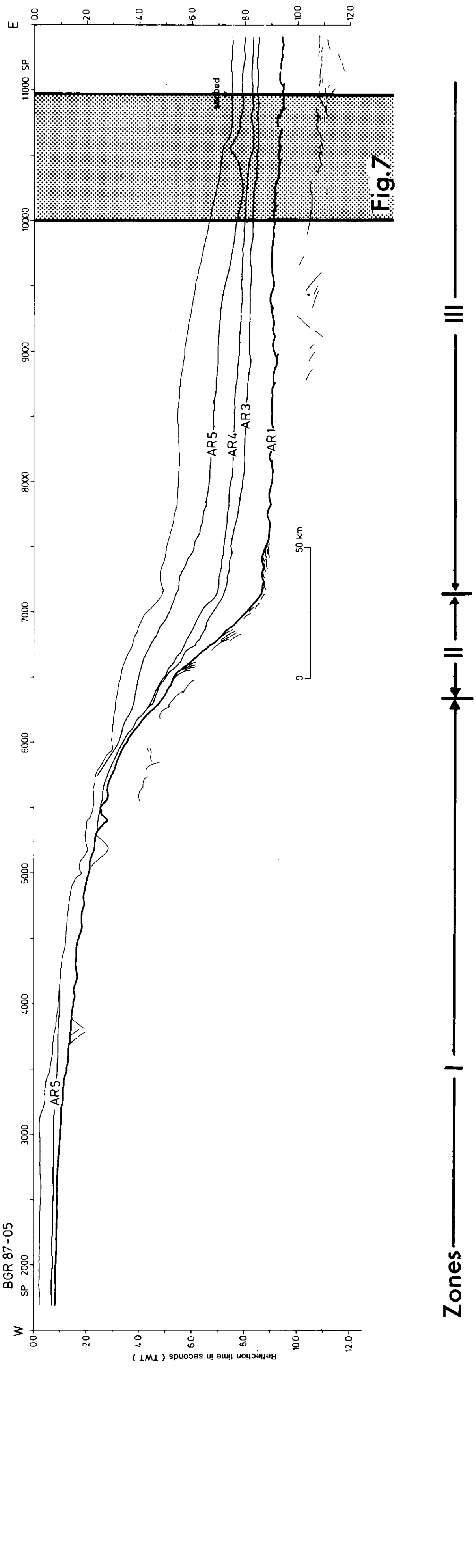

Fig. 6. Interpretation of reflection seismic line BGR 87-05. AR1–5 are regional unconformities. Location on Fig. 1.

Structural units showing similar geometries and seismic characteristics as the dominant structural feature of zone II off Argentine have been observed on many divergent margins (Hinz, 1981; Mutter, Talwani & Stoffa, 1982; Hinz & Krause, 1982; Smythe, 1983; Roberts, Backman, Morton, Murray & Keene, 1984; White et al., 1987; Hinz, Mutter, Zehnder & NGT Study Group, 1987; Skogseid & Eldholm, 1987; Larsen & Jakobsdottir, 1988; Austin et al., 1990). DSDP Leg 81, ODP Legs 104, 152 and 163 drilled into the seaward-dipping wedges and demonstrated that they consist of basaltic flows and interlayered volcaniclastic sedimentary layers (Roberts et al., 1984; Eldholm et al., 1987) Leg 152 Shipboard Party, 1994 (Larsen et al., 1994). The commercial well AC-1 drilled into the feather edge of the wedge of seaward-dipping reflections underlying the conjugate southwestern African margin (Austin & Uchupi, 1982) and encountered 692 m of mainly basic lavas (Gerrard & Smith, 1983). Rabinowitz and LaBrecque (1979) described a distinct magnetic anomaly which they called Anomaly G (Figs 1 and 17) that coincides with the feather edge of the seaward-dipping wedges underlying both the Argentine and the conjugate southwestern African continental margins. They interpreted Anomaly G as an edge effect anomaly between oceanic crust juxtaposed against continental crust. Gerrard and Smith (1983) suggested that the source of Anomaly G are flows and sills overlying continental basement. This interpretation implies that the anomaly pattern interpreted as M5 to M13 by Rabinowitz and LaBrecque (1979) was not generated by simple seafloor spreading.

Figure 17 shows the magnetic anomalies at the continental margin of Argentine demonstrating that whenever magnetic Anomaly G is well developed it coincides with the prominent wedge of seaward-dipping reflectors. Figure 18 shows a magnetic model for the wedge of seaward-dipping reflectors along line BGR87-03. We assigned a magnetization value to the source body that is in the range of the magnetizations measured for basalts from ODP Site 642E of Leg 104 on the Vring Plateau (Schönharting & Abrahamsen, 1989; Schreckenberger, 1997). The direction of the remanent magnetization (inclination -61°, declination 0°) at the time of the formation of the sequence of seaward-dipping reflectors was calculated using the present latitude of the survey area, because the paleo-position of South America in Early Cretaceous times (Van der Voo, 1993) was not significantly different from today. Post-emplacement rotation of the SDRS in the order of 20° caused a slightly steeper inclination (-66°) and a modified declination (40°) of the remanent magnetization vector.

The positive magnetic anomaly G on line BGR87-03 is located within a long-wavelength negative trend of the magnetic field. Because of the lack of detailed information about regional and deep crustal magnetizations, we modelled only the local positive anomaly on line

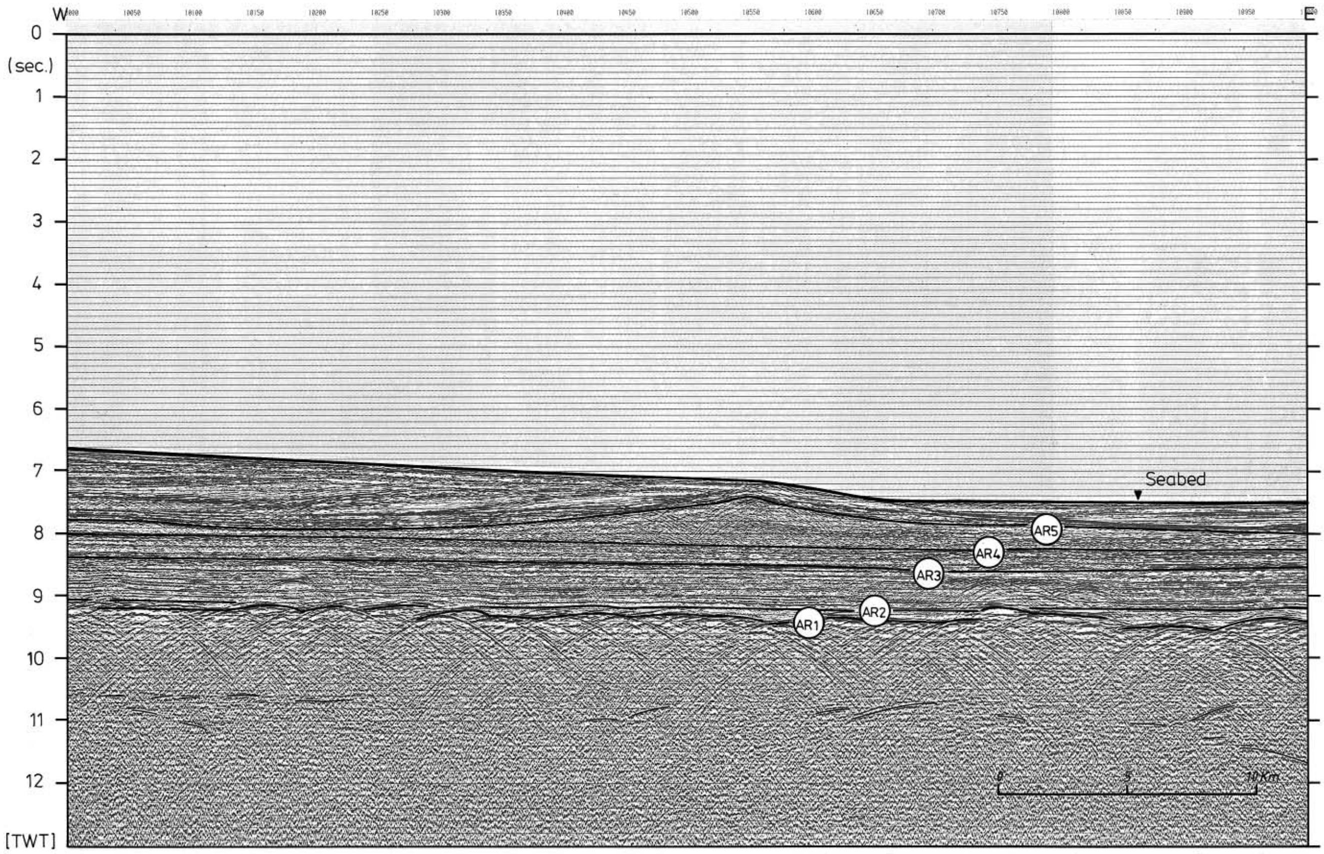

Fig. 7. Interpreted section of stacked multichannel reflection seismic profile BGR 87-05 showing inferred bottom current controlled deposits above unconformity AR3, and a giant dune-like feature above unconformity AR4 described in the text. Location on Fig. 6.

BGR87-03 and made no attempt to fit the body to the regional trend of the data. The magnetic model calculation (Fig. 18) shows that the source body coincides with the major portion of the SDRS and Schreckenberger (1997) shows that this statement also applies to the SDRS on line SO85-06 (Fig. 17). The westernmost and oldest unit of the SDRS on line BGR 87-03 (SP 3000-3500) however, appears to cause no magnetic anomaly and is not included in the model body. We explain this with either alternating polarities of flow sequences due to magnetic reversals or by weak magnetizations, similar to those of the Lower Volcanic Unit (LVU) encountered at ODP Site 642E. There, the LVU contains only very small amounts of magnetic minerals (Schönharting & Abrahamsen, 1989). The steep transition in the thickness of the magnetic source body at SP 4400 fits fairly well to the termination of the major SDRS from where east of SP 4400 a thin magnetic layer represents the averaged magnetization of normal oceanic crust.

Anomaly G is poorly developed on line BGR 87-02/SO85-M004 and south of 43°S, where successively overlapping wedge-shaped sequences characterized by short seaward-dipping reflections are present (Fig. 16). Our preferred explanation for the poor development of Anomaly G south of 43°S is, that the formation of the SDRS was episodic, and that the episodically emplaced and overlapping volcanic sequences recorded alternating polarities of the earth's magnetic field in their thermoremanent magnetization. But other circumstances that led to the formation of the weakly magnetized SDRS cannot be excluded. Reconstruction poles for the earliest time of the opening of the South Atlantic (Rabinowitz & LaBrecque, 1979; Nürnberg and Müller, 1991) indicate that propagation of rifting to the north combined with frequent reversals might explain the observed variability of Anomaly G along the Argentine margin.

We assume that the major portion of the wedge shaped sequence characterized by a distinct seaward-dipping reflection pattern developed immediately prior to the earliest stage of seafloor spreading in a subaerial environment, whereas the overlapping wedge-shaped sequences characterized by short seaward-dipping reflections may have been emplaced in greater water depths and possibly along an already developed spreading ridge.

The seaward edge of the subaerially emplaced voluminous extrusives lies about 100 km landward of magnetic anomaly M4 (about 126 Ma, Late Hauterivian, Kent & Gradstein (1986) time scale) at 44°S, but

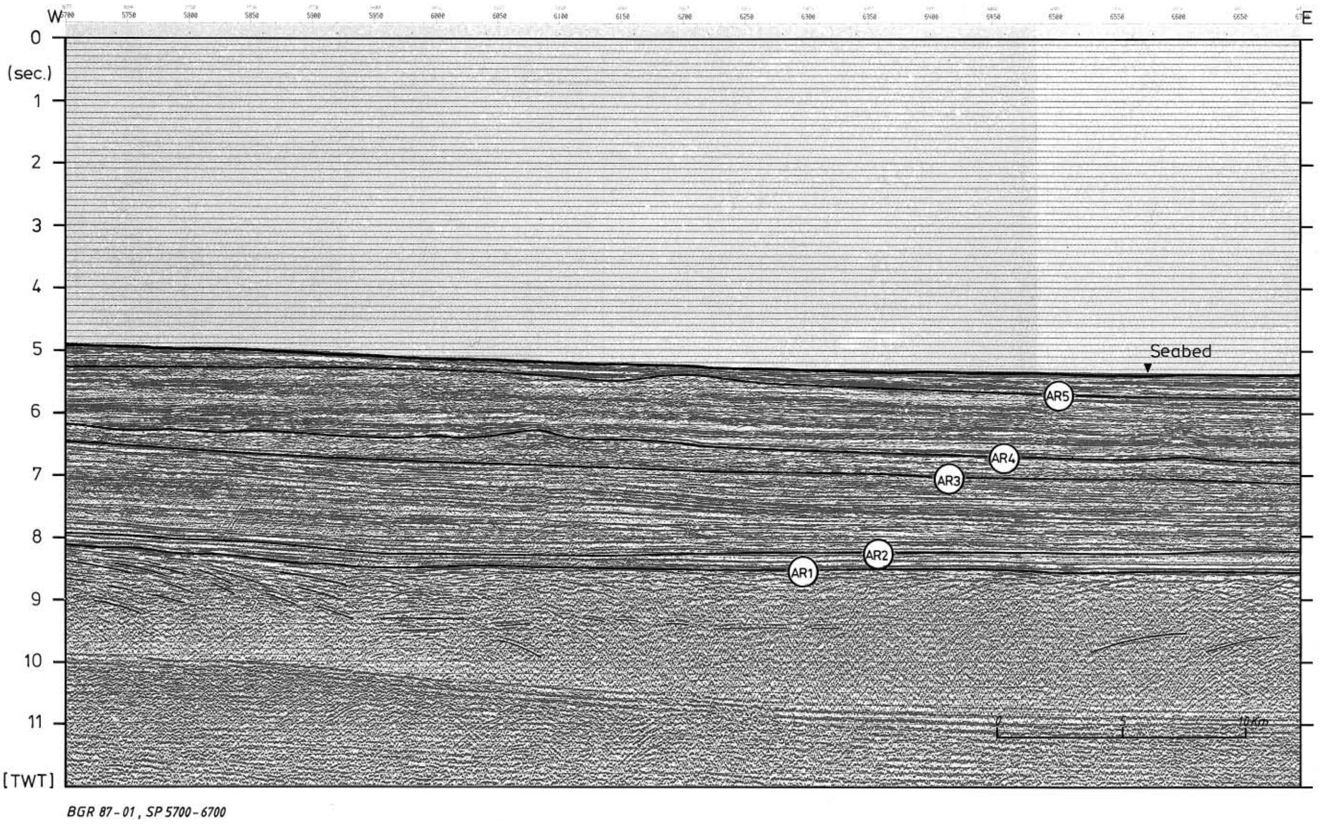

Fig. 8. Interpreted section of stacked multichannel reflection seismic profile BGR 87-01 showing bottom current-controlled deposits including mounds within the post-AR3 succession. Location on Fig. 4.

approaches towards magnetic lineation M3 (125 Ma) at 35.5°S, which might suggest that subaerial emplacement along the margin was diachronous (Fig. 9).

Zone II merges into Zone III (Fig. 9) which begins at the seaward edge of the well developed wedge of seaward-dipping reflections and extends to a region where magnetic anomaly M0 (118.7 Ma, Earliest Aptian, Kent and Gradstein (1986) time scale) has been identified (LaBrecque & Rabinowitz, 1979). A sedimentary succession with thicknesses varying between 2 and 4 s, i.e. 4000–6000 m (Figs 4, 6, 10 and 11) overlies the oceanic crust that accreted at slow rates (half rates 15–20 mm/a). The surface of the oceanic crust within Zone III is smooth to flat and represented by a strong reflector with several offsets ranging from 0.1 to 0.4 s (Fig. 19). Some of these offsets may represent fault displacements because they occur at the upward projection of elongated and steeply dipping reflection events in middle and lower crustal levels. Others are interpreted as scarps presumably representing west-facing edges of basaltic flows.

Zone IV covers the oldest portion of the CMQZ. Its basement architecture differs from Zone III by a more irregular relief and poor intracrustal reflectivity. The crust-mantle boundary is poorly imaged. It appears that the basement of Zone IV has been affected by extensional deformation.

5. Volcanic activity during breakup

Our geophysical studies on the Argentine continental margin, of which we have described the principal findings, demonstrate that its formation was associated with an excessive episode of volcanism represented by a voluminous wedge of seaward-dipping reflectors comprising our structural Zone II. This episode followed the Late Jurassic through Early Cretaceous rifting phase and was associated with strong uplift resulting in regional peneplanation.

Goncalves de Souza (1991) and Hark and Hinz (1995) demonstrate that the huge volumes of volcanic material exists also beneath the outer continental margins of Uruguay and southern Brazil, i.e. it extends from the Falkland Plateau at 48°S over a total distance of 3500 km up to the Vitoria–Trinidade seamount chain at 21°S (Fig. 20).

We estimate a minimum total subaerially extruded rock volume of 1.5×10^6 km^3 for this South American offshore volcanic construction which was emplaced on an area of approximately 550,000 km^2. This estimate of the extrusive rock volume does not include the probably coeval volcanism of the Paraná continental flood basalts (CFB). The main emplacement of this voluminous volcanic body was probably diachronous decreasing rapidly

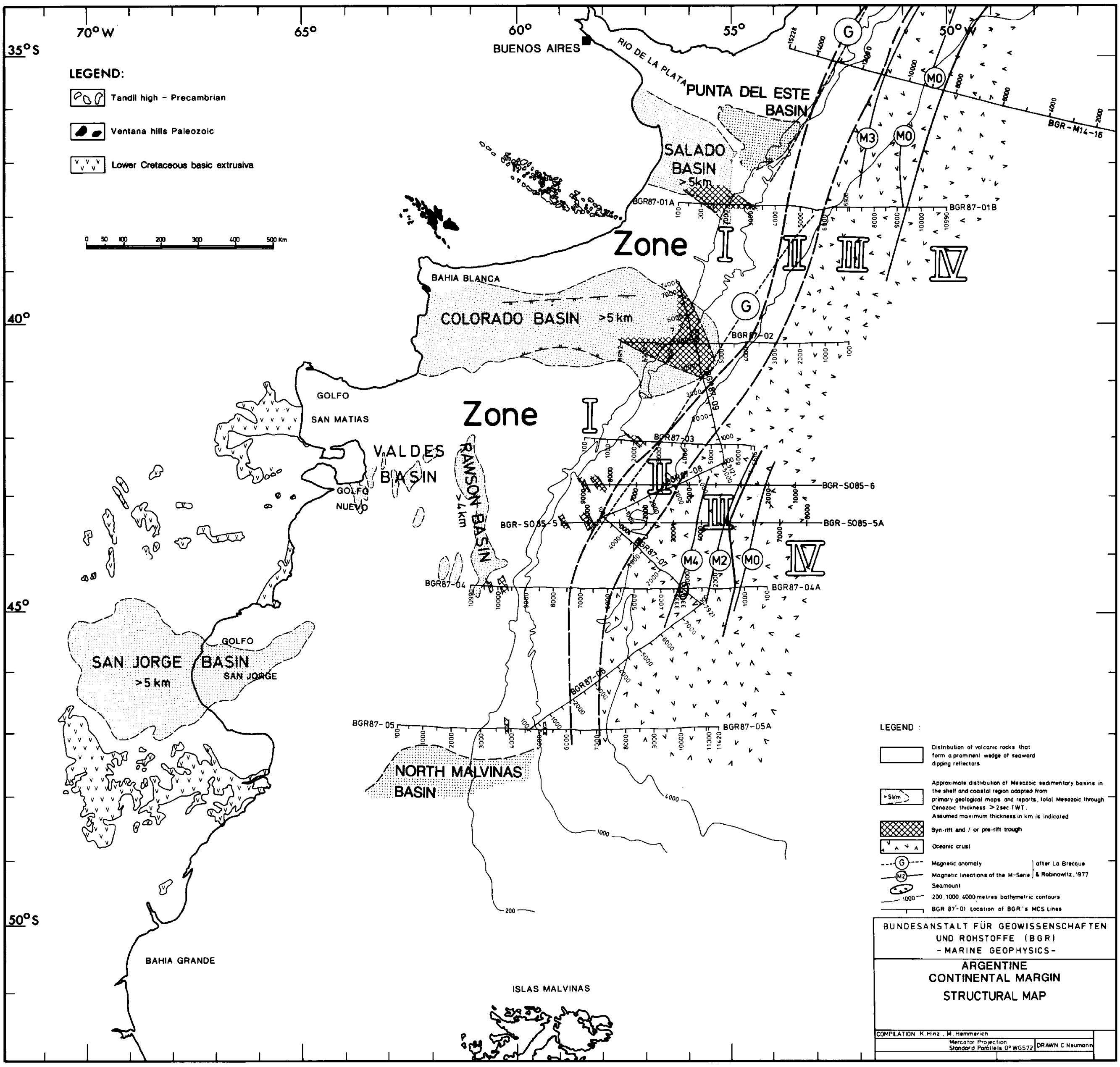

Fig. 9. Elements of the Argentine continental margin grouped into four structural zones discussed in the text. Also shown is the approximate distribution of Mesozoic sedimentary basins on the inner shelf region from published work.

prior to magnetic anomaly M4 (about 126 Ma) at the Argentine continental margin, but prior to magnetic anomaly M3 (about 125 Ma) at the continental margin of Uruguay. A comparable volcanic structure concerning the architecture, seismic characteristics and time of formation exists at the conjugate continental margin of Namibia and South Africa (Gladczenko et al., 1996; (Fig. 20)).

The volume of 1.5×10^6 km^3 and an assumed duration of 5 Ma implies an average rate of extrusion of 0.3 km^{3}a, or if symmetric 0.6 km^{3}a. This is about 15 times larger than the estimated average rate of extrusion for the past 1100 years on Iceland (0.038 km^{3}a) (Thorarinsson, 1968) and for Tristan da Cunha (0.03 km^{3}a) (Richards, Duncan & Courtillot, 1989), respectively. However, magnetic model calculations suggest that most of the lava successions, forming the younger (seaward) part of the wedge-shaped volcanic structure beneath the Argentine continental margin north of 43°S, accreted within a normally magnetised interval, e.g. between magnetic chrons M4 and M12 during a maximum of less than 2 Ma. An assumed duration of 2 Ma for the emplacement of the

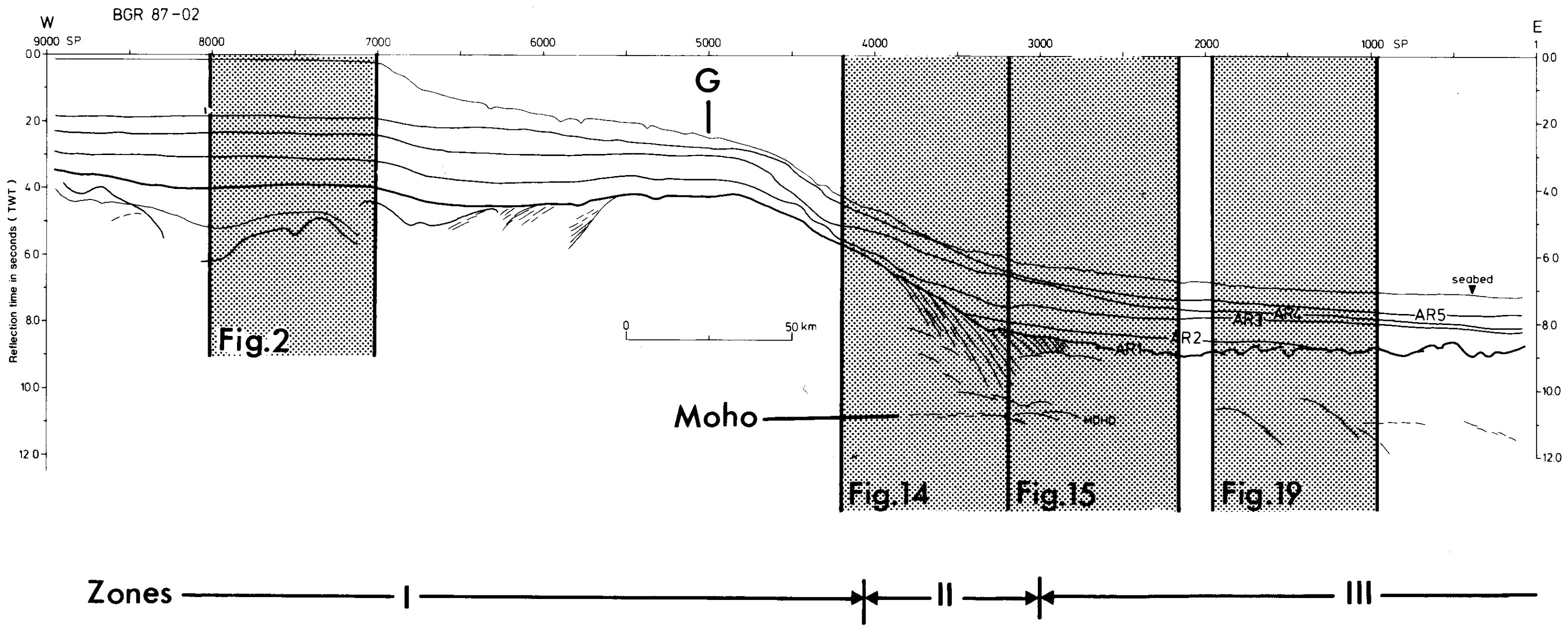

Fig. 10. Interpretation of reflection seismic line BGR 87-02. AR1–5 are regional unconformities. Location on Fig. 1.

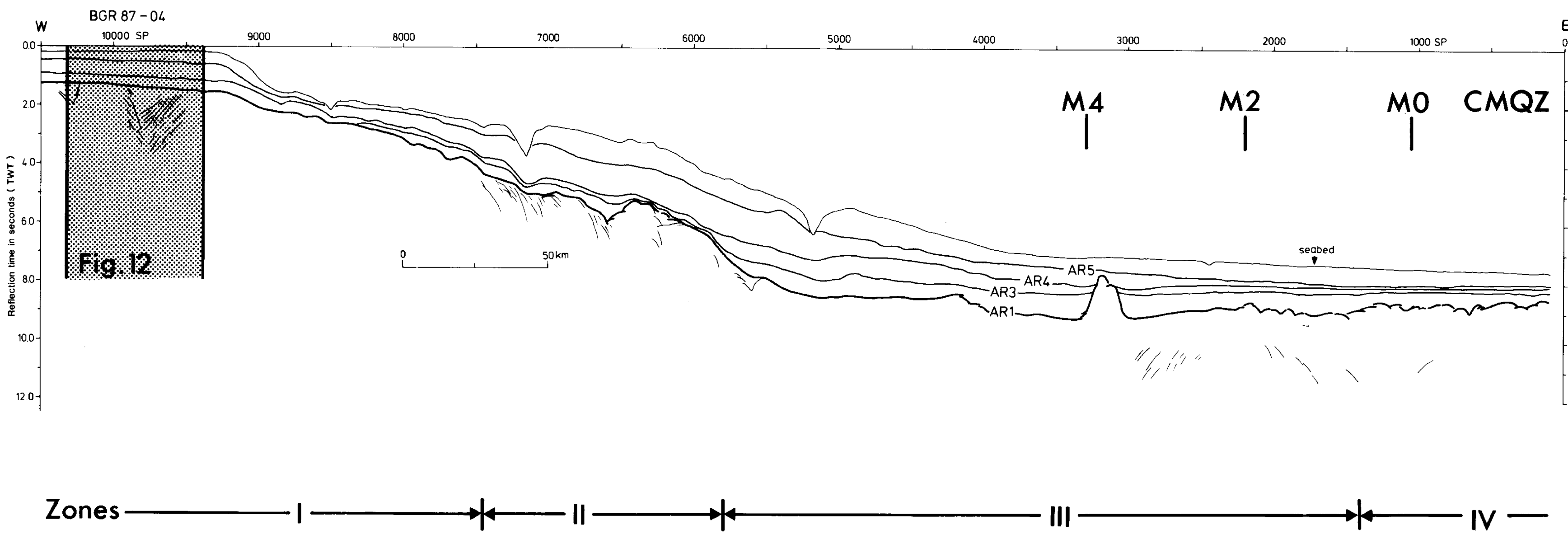

Fig. 11. Interpretation of reflection seismic line BGR87-04. Location on Fig. 1.

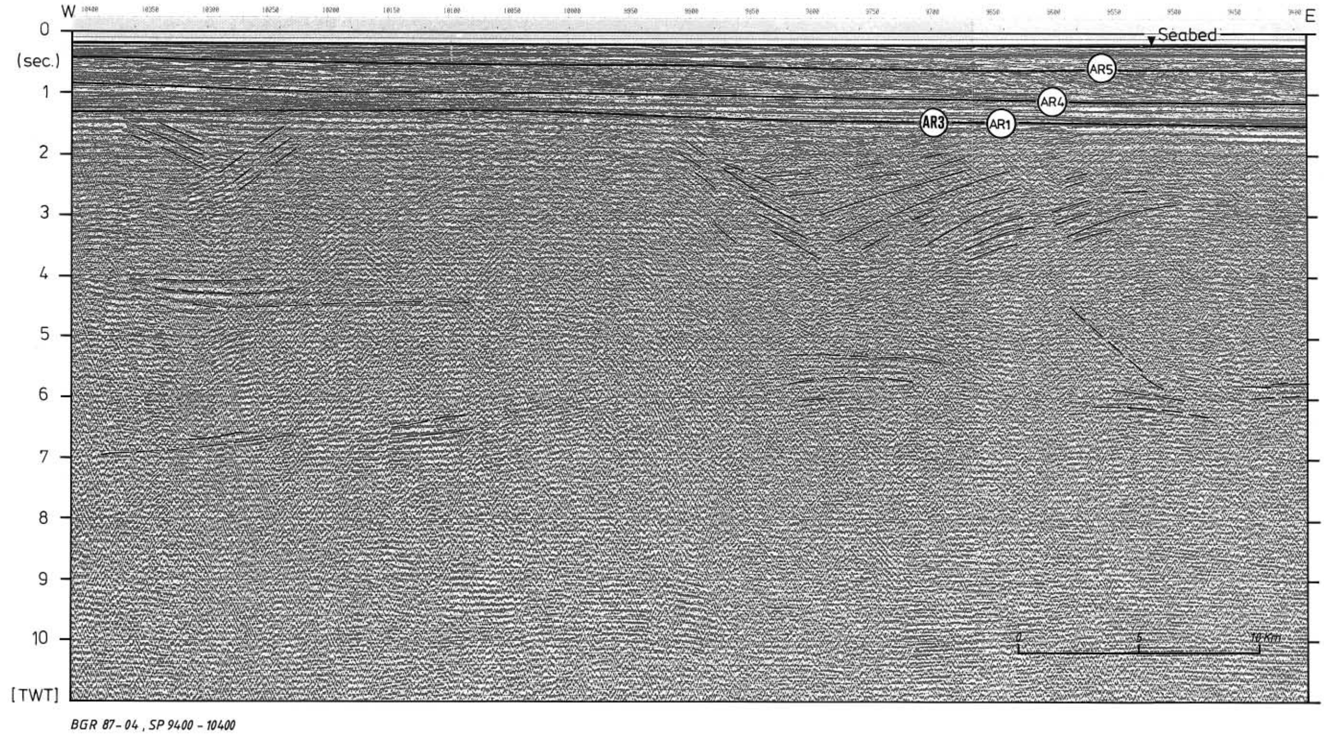

Fig. 12. Interpreted section of stacked multichannel seismic profile BGR 87-04 showing possible syn-rift or pre-rift features described in the text. Location on Fig. 11.

main SDRS implies an average rate of extrusion of 0.21 km^3 per Ka per km rift length, or if symmetric, 0.42 km^3 per Ka per km rift length; this is in the range estimated for the SDRS of the North Atlantic volcanic margins (Eldholm & Grue, 1994).

There are currently three competing hypotheses for the origin of the volcanic margins: White and McKenzie (1989) argue that excessive igneous activity is due to 'passive' rifting over a mantle plume and its large mushroom-shaped head enhancing decompression melting and increased volcanism. From this model it follows that volcanism should be most intense over the plume and decreases with distance from the plume. Mutter, Buck and Zehnder (1988) proposed small scale convection at a pre-existing and relatively sharp plate boundary as the mechanism for producing thick volcanic constructions. This model does not require influx from an external source other than a stronger mantle convection, initiated by a lateral temperature gradient between the relatively cold continental lithosphere and the warm mantle rising into a zone of lithospheric rupturing. Campbell and Griffiths (1990) and Duncan and Richards (1991) proposed a model of decompression melting within a rising plume head resulting in a rapid and vigorous burst of volcanism. The episode of massive igneous activity is considered a transient effect of the initial plume head. The hot-spot and plume-head models imply that the mantle temperature should decrease radially from the plume, and this in turn predicts that the volume of extrusive rocks will decrease with distance. On the contrary, we observed that the wedge of seaward-dipping reflectors along the South American continental margin extends only 800 km to the north from the reconstructed hot-spot position at 120 Ma (Duncan, 1984), but extends 2600 km to the south from this position.

6. Temporal variability in generation of oceanic crust

We refer to a new and intriguing observation of isochronous changes of the seismic images of the early Cretaceous through Early Tertiary old oceanic crust of the South Atlantic (Hinz et al., submitted). The seismic images along our flow-line transects (Fig. 20), located north and south of the Walvis Ridge and the Rio Grande Rise, which are interpreted as volcanic trails from the Tristan da Cunha hotspot (Richards et al., 1989), are heterogeneous and variable suggesting both distinct and gradational changes of the internal structure of the oceanic crust in time and space. Due to scarcity of reliable seismic velocity information from refraction and wide-angle reflection data and some ambiguity of the internal velocities derived from NMO velocities we used primarily the following reflection characteristics to classify the oceanic crust along our flow-line profiles:

- Topography and reflectivity of the basaltic basement

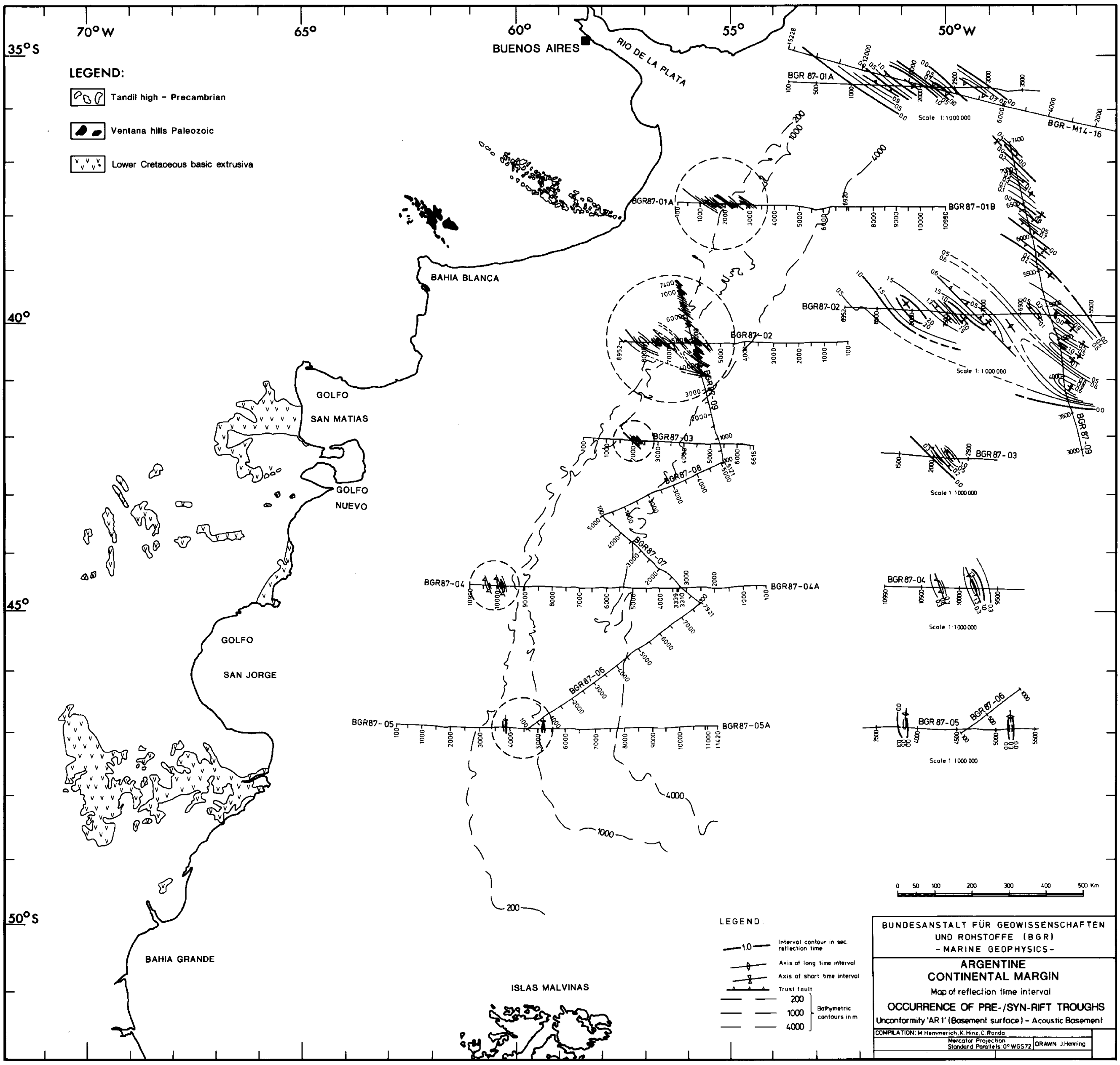

Fig. 13. Occurrence of recognized syn-rift and possible pre-rift troughs, and the thickness (twt) of their sedimentary infill, enlarged on right side.

surface and its depth in comparison to the Parsons and Sclater (1977), Renkin and Sclater (1988) predicted elevation.

- Intensity and kind of reflectivity in upper, middle and lower crustal levels.
- Intensity and nature of reflectivity near the inferred crust-mantle boundary.

We can demonstrate the presence of four major seismic crustal categories and several gradual changes within the Cretaceous-aged oceanic crust of the South Atlantic on the basis of the above seismic parameters. These four major crustal categories are:

Crustal category A comprises the prominent wedge of seaward-dipping reflectors described previously (Figs 5, and 14–16).

Crustal category B has a small-scale irregular basement relief. Coherent reflectivity is very low in lower crustal levels (Fig. 21).

Crustal category C has a strong reflective and irregular basement relief with offsets in the range

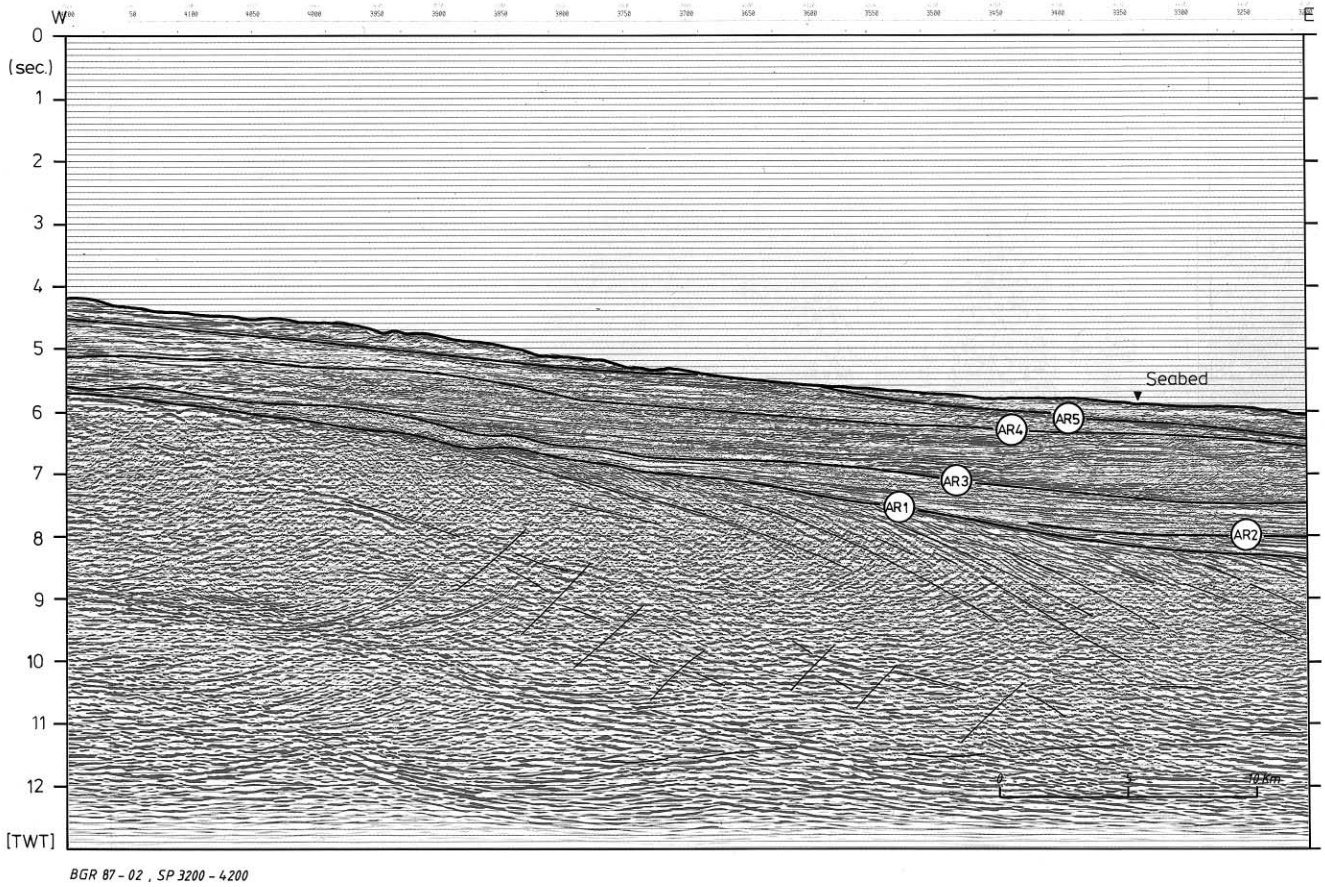

Fig. 14. Interpreted section of stacked multichannel reflection profile BGR 87-02 showing the landward portion of the prominent wedge of seaward-dipping reflectors. Location on Fig. 10.

of 100–500 m. The shallow crust contains some subhorizontal reflection elements, and the middle crust is seismically almost transparent. The lower crust and possibly the uppermost mantle is represented by a reflective sequence, 1 to 1.5 s thick, with accentuated dipping (approximately 20° to 30°) reflections toward the spreading axis (Fig. 22). *Crustal category D* is characterized by a flat to smooth basement surface and a sequence of seaward-dipping reflectors beneath. This upper-crustal sequence resembles the SDRS of volcanic margins (category A), but its thickness is much smaller (0.3–0.8 s). Typically the lower crust exhibits high-amplitude reflectivity without a preferred pattern. This highly reflective lower-crustal sequence is up to 1.5 s thick. Its upper boundary against the mostly transparent middle crust has a variable relief. Downward termination of the reflectivity pattern is rather abrupt between 9 and 10 s in the Angola and Brazil Basins (Fig. 23). Elongate dipping reflections traversing from the upper crust through the middle crust into the lower-crustal reflective sequence are very seldom imaged in those areas along our flow-line traverses where seismic crustal categories D and C prevail. Wide-angle reflection/refraction experiments from the Angola Basin yielded thicknesses for the oceanic crustal categories C and D of 8 and 9 km, respectively.

It has been argued by Mutter and Karson (1992) among others, that the strong lower-crustal reflectivity is primarily the expression of mechanical processes of deformation. Unlike Mutter and Karson (1992), we believe that strong lower-crustal reflectivity, typically of our Cretaceous-aged crustal categories C and D of the South Atlantic, represents magmatic layering originally produced by processes in the magma chamber, because it is hard to understand how deformation could produce shear and/or fault zones throughout the lower oceanic crust without generating any corresponding structures in the upper and middle crust.

Our preferred explanation of the strong lower-crustal reflectivity of the Cretaceous-aged crustal categories C and D receives some support by the results of seismic waveform modelling of some ophiolite complexes, which suggest that layering of mafic and ultramafic cumulates

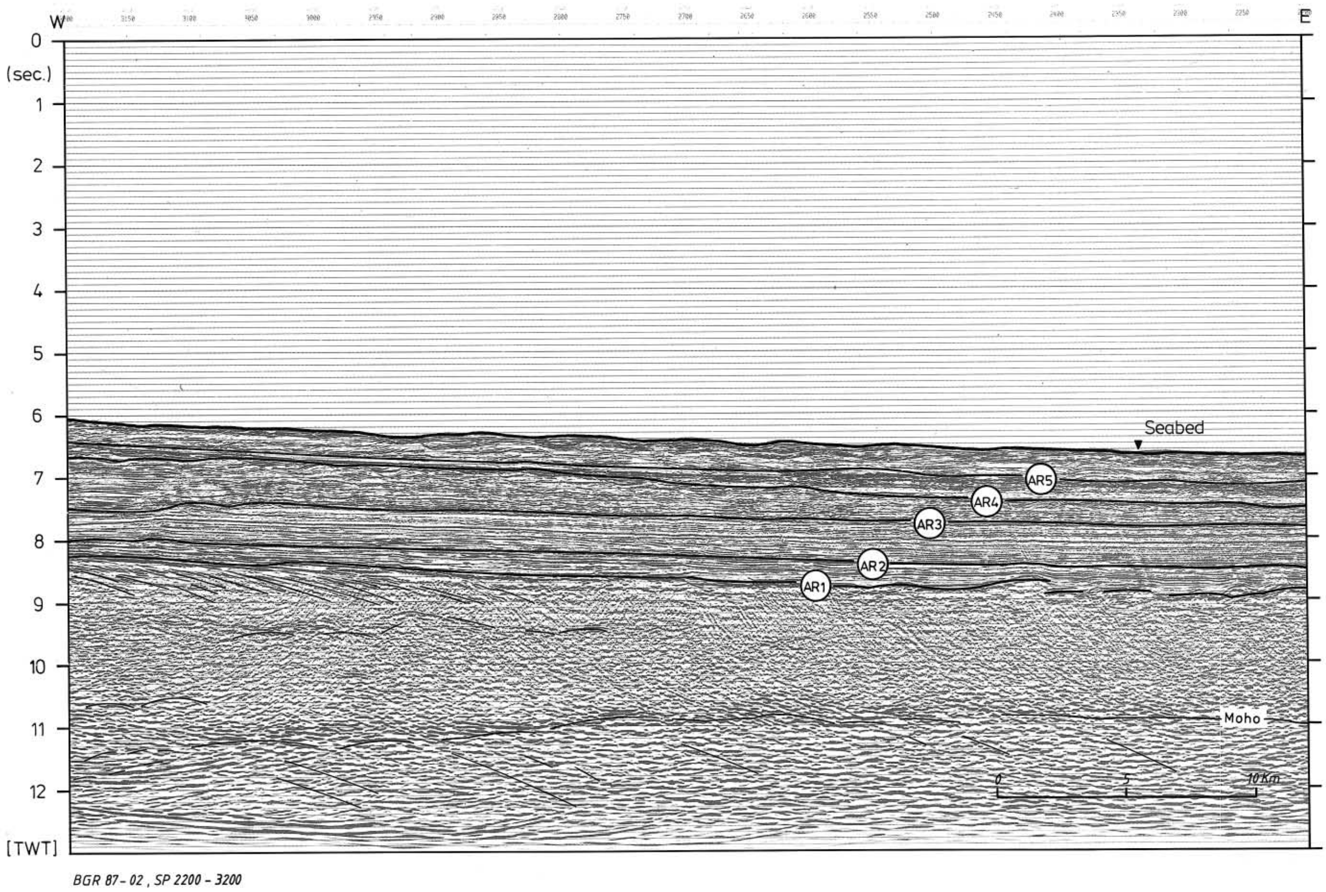

Fig. 15. Interpreted section of stacked multichannel reflection seismic profile BGR 87-02 showing the seaward termination of the prominent wedge of seaward-dipping reflections. The inferred crust-mantle boundary at approximately 11 s (twt) deepens landward under the wedge of seaward-dipping reflectors. Location on Fig. 10.

could generate layered crustal reflectivity in the lower oceanic crust (Collins, Brocher & Carson, 1986; Kempner & Gettrust, 1982a,b; Christensen & Smewing, 1981).

Principal ophiolite types which are known (Nicolas, 1989) are the Harzburgite Ophiolite Type (HOT) and the Lherzolite Ophiolite Type (LOT). The HOT-type is characterized by a thick layered gabbro section and ultramafic intrusions suggesting intensive magmatic activity in the upper mantle and a larger degree of melt extraction than the LOT-type. The scarcity of layered gabbros in the crustal section of the LOT-type suggests a cooler regime (Nicolas, 1989).

We tentatively correlate the defined seismic crustal categories C and D including the gradual changes between these categories with the HOT-type. Seismic category B is correlated with the LOT-type and/or the 'discontinous magmatic crust' (Cannat, 1993) accreted during moderate magma (heat) supply episodes and/or during poor magma (heat) supply episodes along the mid-ocean ridge system, respectively.

If we are correct, there are several import implications for the origin and development of the oceanic crust of Cretaceous age in the South Atlantic:

- The distribution of oceanic crust, comprising crustal categories B, C and D and gradual changes between these categories is systematic and isochronous (Fig. 20) within the surveyed crustal segments and trends normal to the predicted trace of Tristan da Cunha hotspot.
- These observations suggest, that there was some form of episodicity of rich magma (heat) supply and poor to moderate magma (heat) supply in the accretionary processes at the pre-existing mid-ocean ridge of the South Atlantic during Cretaceous time.
- In the Brazil Basin and the conjugate Angola Basin oceanic crust, characterized by the form of reflectivity of categories C and D described before, accreted during two episodes of inferred rich magma supply alternating with inferred episodes of poor to moderate magma supply (crustal category B). Assuming an averaged spreading for the CMQZ the episodes of inferred rich magma supply are: a period during the Albian, i.e. about 113–97 Ma (Kent and Gradstein, 1986), and an

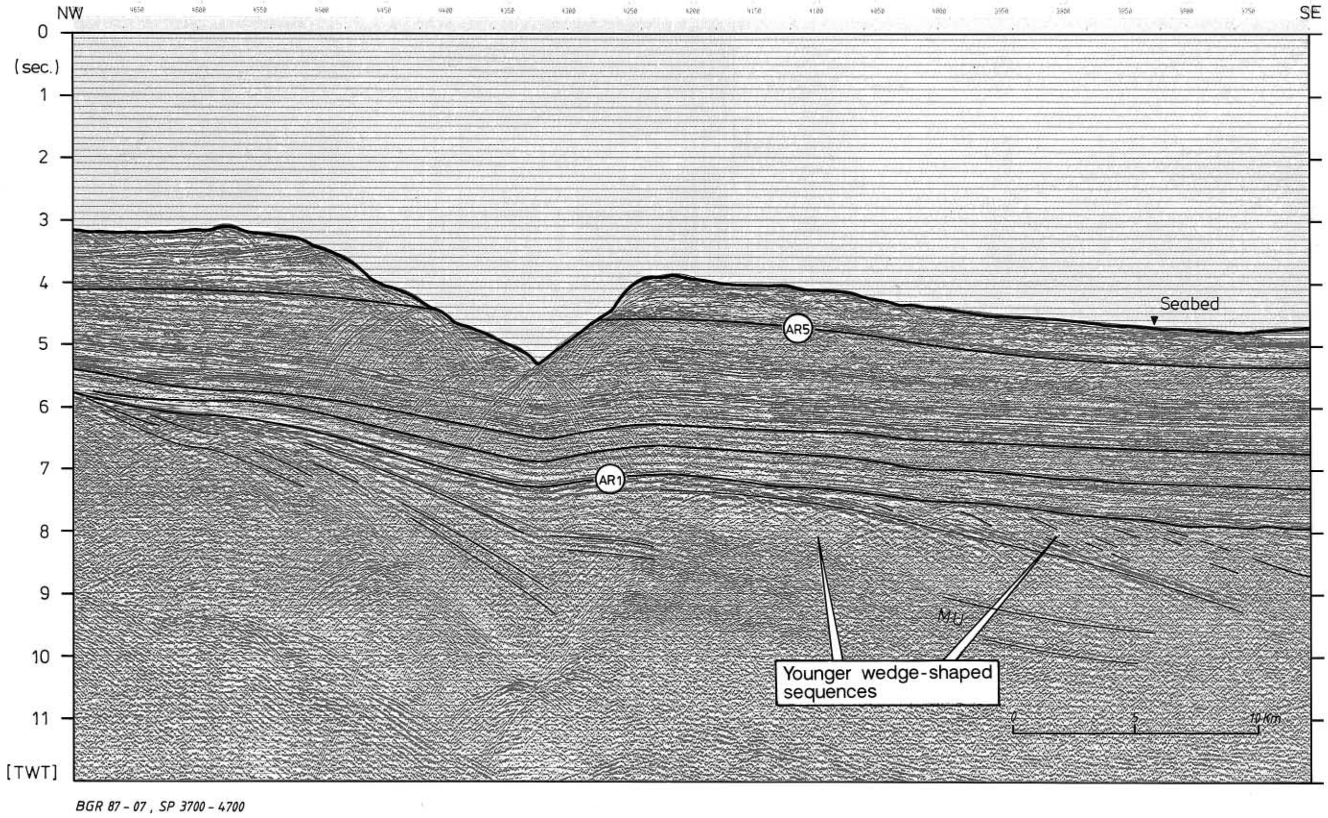

Fig. 16. Interpreted section of stacked multichannel reflection seismic profile showing successively overlapping wedge-shaped sequences discussed in the text. The line segment illustrated is from profile BGR 87-07. MU refers to multiple reflections.

episode during the Latest Cenomanian/Earliest Turonian through Early Campanian, i.e. about between 90–81 Ma.

- In the Argentine Basin and in the conjugate Cape Basin there is clear evidence for one episode of rich magma supply during the Albian through early Campanian, i.e. about between 100–81 Ma.
- Oceanic crust created during post-chron 33r (<80 Ma) times at the South Atlantic mid-ocean ridge system with spreading rates varying between 30–75 mm per year has typically an irregular to strong basement relief and coherent reflectivity is generally low in lower crustal levels and corresponds to crustal category B.

We speculate that regionally hot mantle episodes can better explain the recognized isochronous changes of the Cretaceous-aged oceanic crust instead of an isolated hot-spot, because there is also no distinct change in the width of the Tristan da Cunha hot-spot trail.

7. Conclusion

We have presented new seismic data and geophysical results from the outer Argentine continental margin, and from seismic flow-line transects across the Cretaceous-aged oceanic crust of the South Atlantic.

The results document intense, transient volcanism during Early Cretaceous South Atlantic breakup, emplacing a voluminous volcanic wedge of seaward-dipping reflectors (SDRS) over a distance of 3500 km from 48°S to 20°S on the outer South American continental margin, and on most of the conjugate South African outer continental margin.

Magnetic modeling identified the SDRS as the source of magnetic anomaly G wherever it can be recognized in the study area. We suggest that the high variability of anomaly G over an obviously continuous SDRS along the Argentine margin is caused by northward propagation of rifting at a time of high reversal frequency leading to variations in the polarity of the lavas emplaced at different times. SDRS south of 43°S are different from that in the north as they are less voluminous and do not show significant magnetic anomalies.

We have described isochronous changes in the seismic images of the Cretaceous-aged oceanic crust transects north and south of the Walvis Ridge and the Rio Grande Rise. Zones of thickened oceanic crust characterized by strong lower crustal reflectivity, suggesting accretion dur-

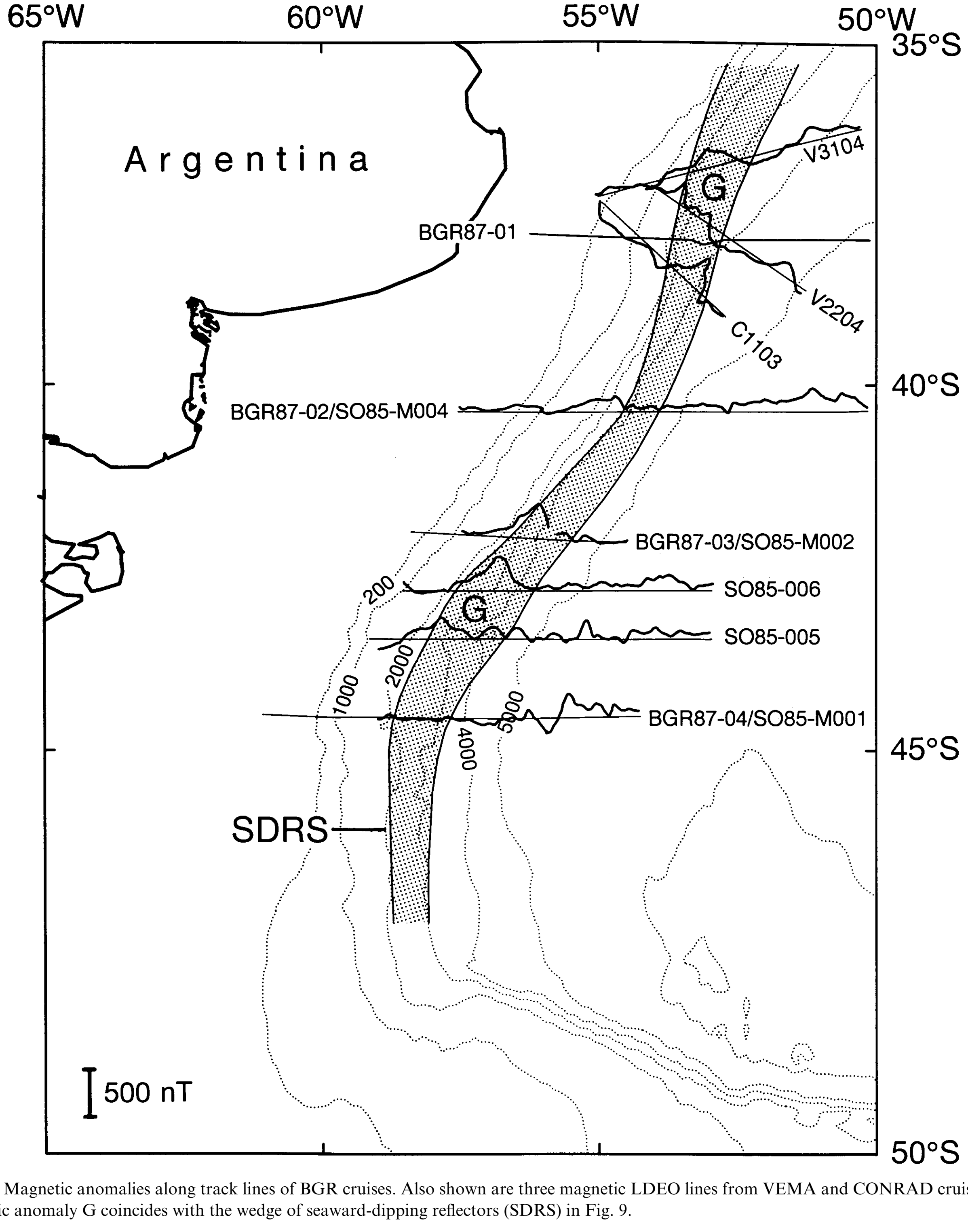

Fig. 17. Magnetic anomalies along track lines of BGR cruises. Also shown are three magnetic LDEO lines from VEMA and CONRAD cruises. The magnetic anomaly G coincides with the wedge of seaward-dipping reflectors (SDRS) in Fig. 9.

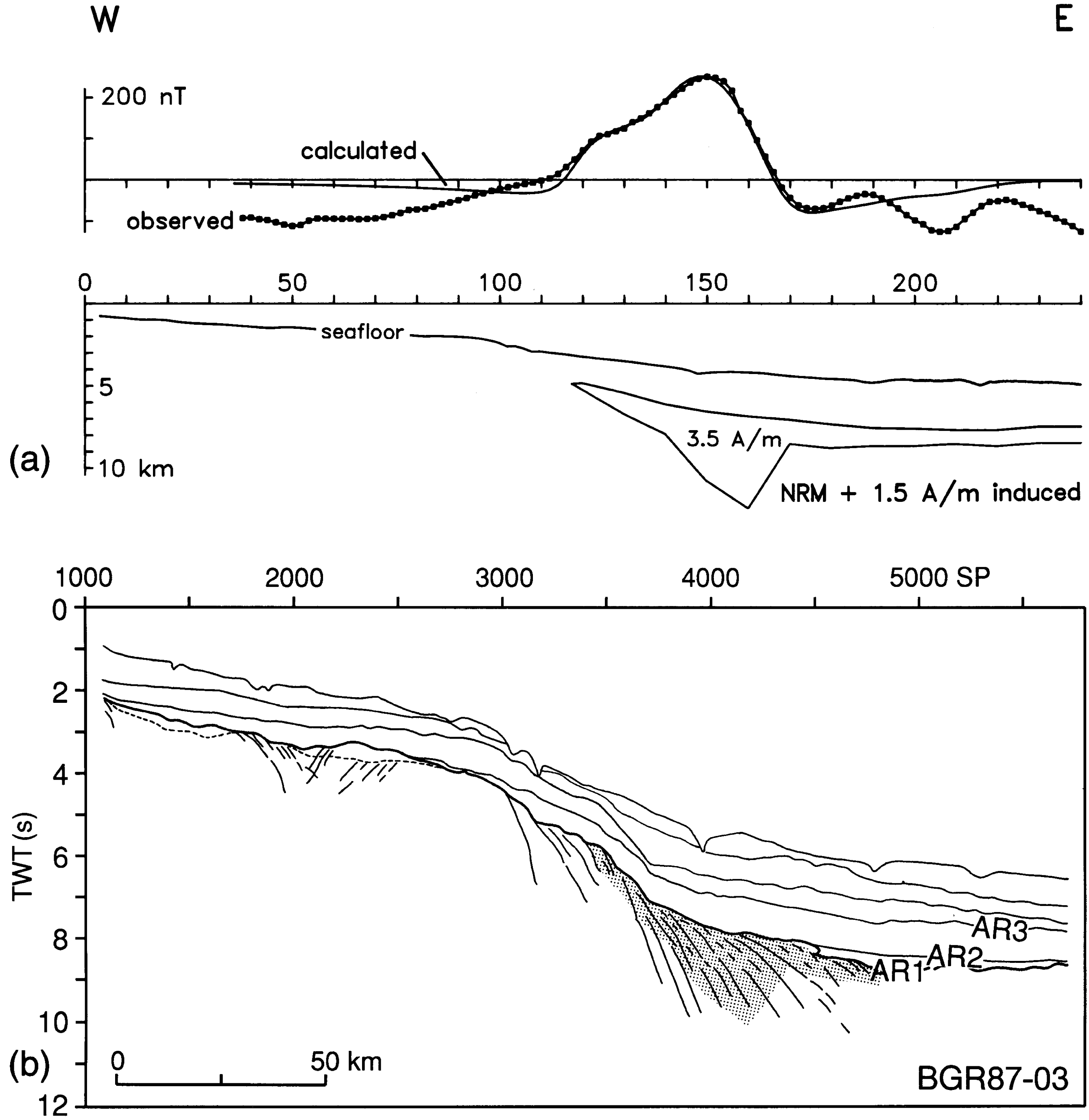

Fig. 18. (a) Two-dimensional model calculation for the magnetic anomaly G on line BGR 87-03 (location see Fig. 17). The source body contains a remanent magnetization of 3.5 Am^{-1}, (inclination $-66°$, declination 40°) and an induced magnetization of 1.5 Am^{-1}. (b)The source body from (a) is shown overlaying the line drawing of the seismic section. The conversion from the depth scale in the model calculation to reflection time in the line drawing was performed using a seismic velocity of 5 km^{-1} for the SDRS.

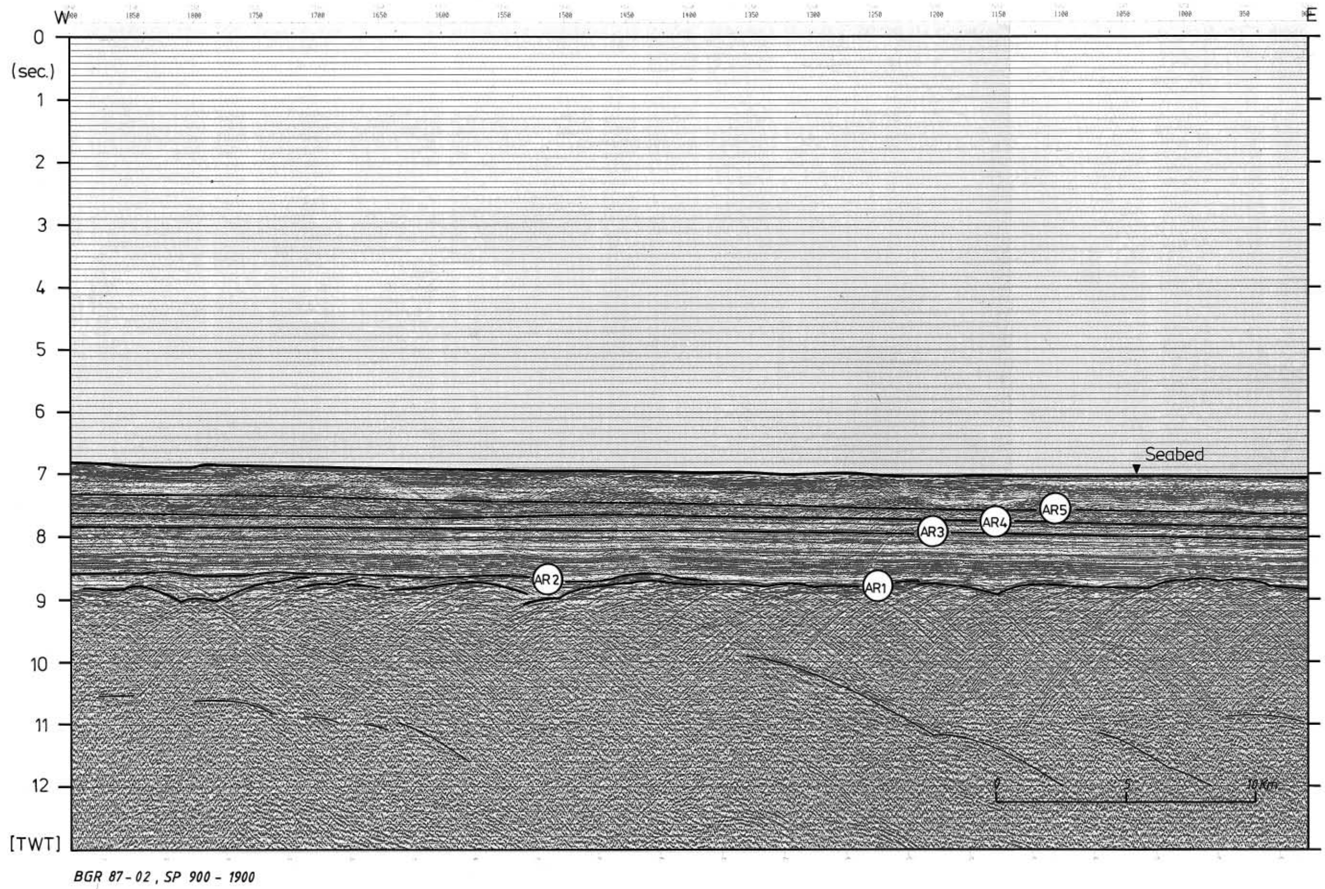

Fig. 19. Interpreted section of stacked multichannel reflection seismic profile BGR 87-02 from structural zone III showing enlongated dipping events in middle and lower crustal levels described in the text. Location in Fig. 10.

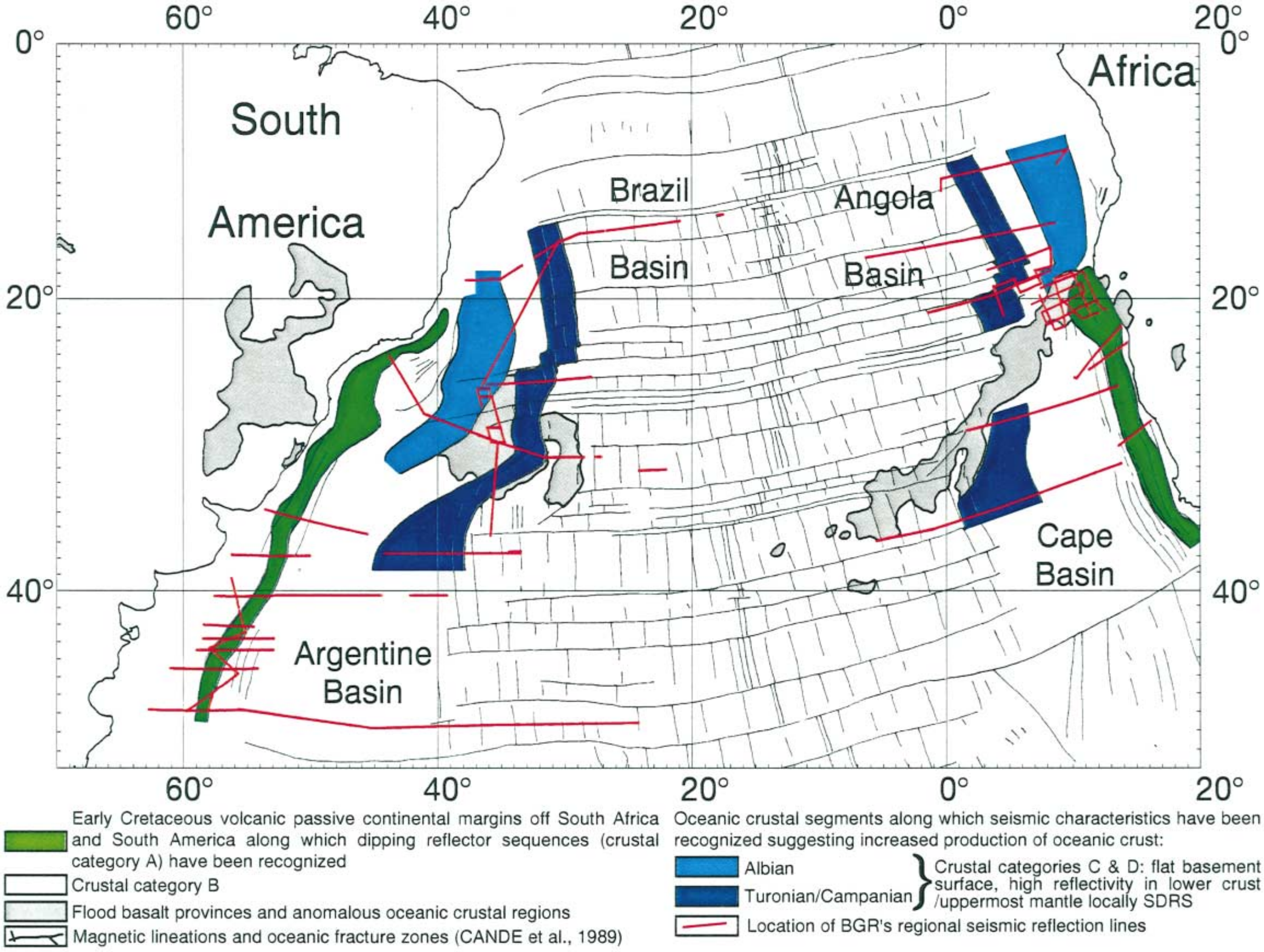

Fig. 20. Distribution of crustal categories A, B, C and D across the South Atlantic. The Paraná and Entendeka continental flood basalt provinces, and the Rio Grande Rise, Walvis Ridge and Agulhas Plateau are indicated in grey and BGR's seismic transects are in red lines. Magnetic anomalies and fracture zones from Cande et al. (1989).

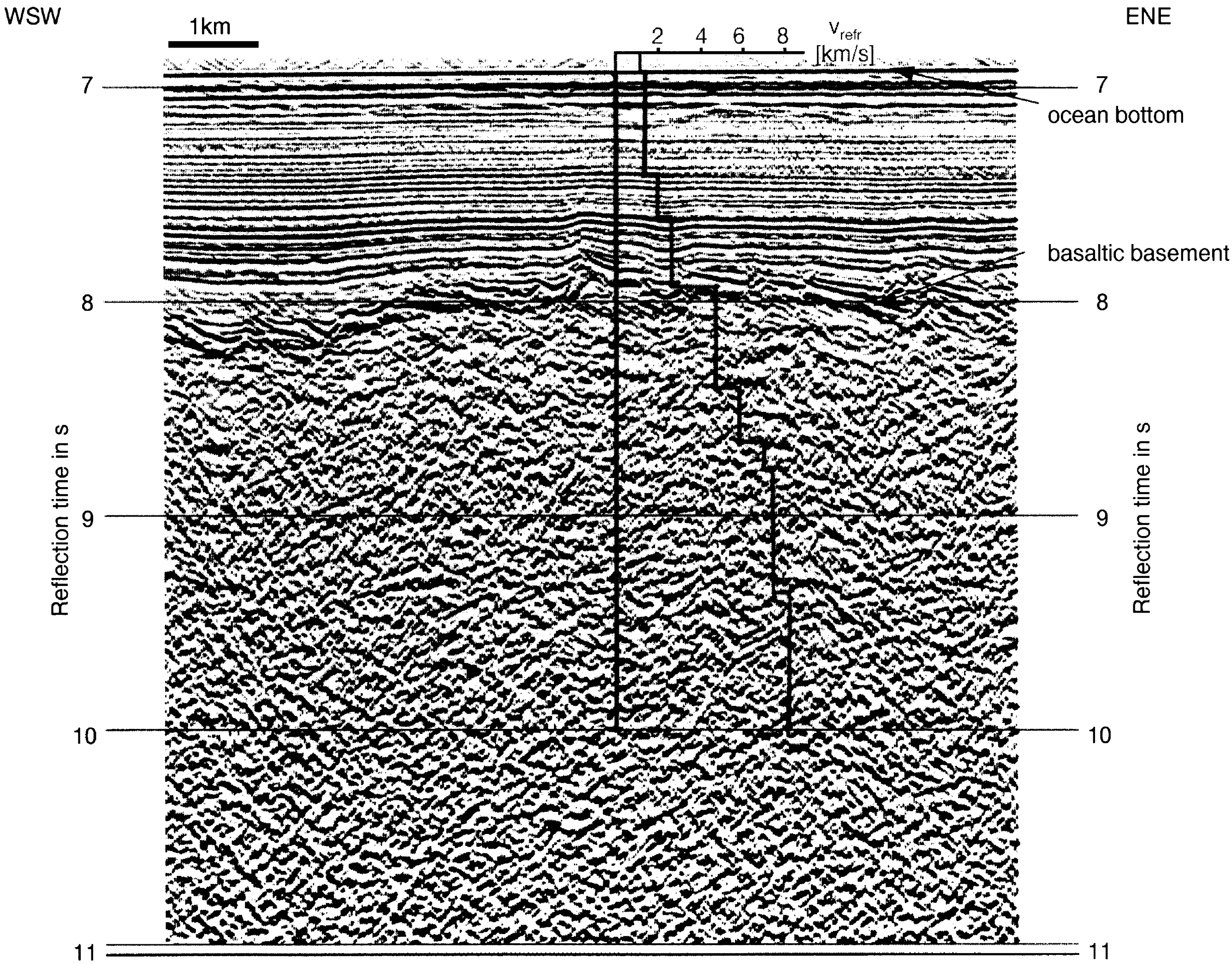

Fig. 21. Typical migrated seismic image of crustal category B. The oceanic basement surface has a small-scale irregular relief, the upper and middle oceanic crust shows a non-coherent reflection pattern. Coherent reflectivity is very low in lower crustal levels; no clear Moho reflection. The illustrated seismic section is from the southern Angola Basin. The velocity-time function derived from results of wide-angle reflection/refraction measurements along the illustrated profile is indicated.

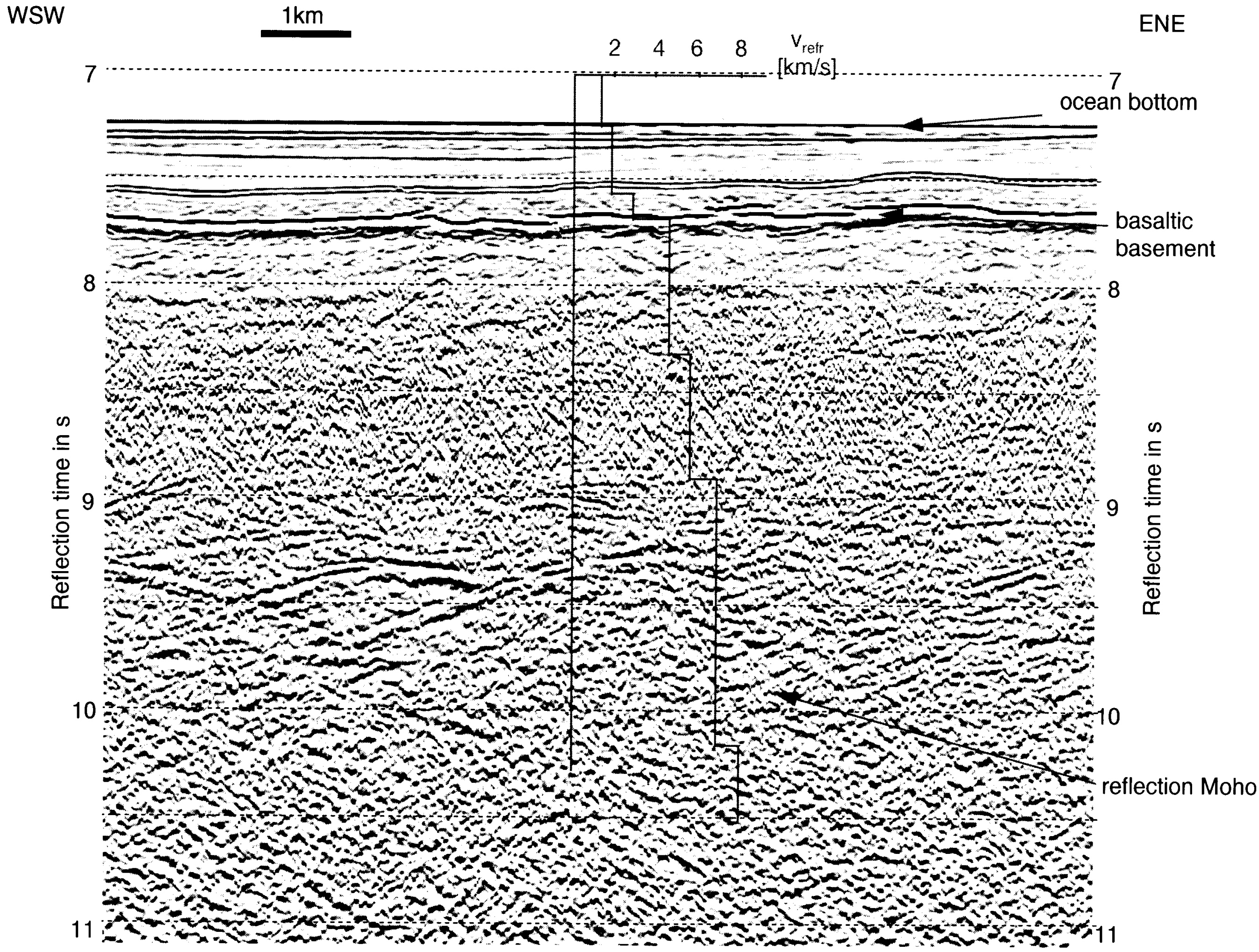

Fig. 22. Migrated seismic image of crustal category C illustrating the major forms of reflectivity described in the text. The illustrated seismic section is also from the southern Angola Basin. The velocity-time function derived from results of wide-angle reflection/refraction measurements along the illustrated section is indicated.

ing high magma (heat) supply episodes along the former spreading ridge, alternate with zones where reflectivity in lower crustal levels of relatively thin (<7 km) oceanic crust is very low. The zones trend normal to the Tristan da Cunha hot spot trail, implying some form of episodicity between rich magma (heat) and poor to moderate magma supply in the accretionary processes at the preexisting South Atlantic mid-ocean ridge during Cretaceous time.

We think that the non-radially symmetric distribution of the SDRS's regarding to the reconstructed position of the Tristan da Cunha hot spot, the apparently diachronous emplacement of the SDRS along the Argentine–Uruguay continental margin, and the isochronous variability of the oceanic crustal structure in the Brazil–Angola and in the Argentine–Cape Basins are difficult to reconcile with an isolated, long-lived mantle plume. We consider temporal convective instability originating from the thermal boundary layer and caused by deep and relatively sharp lithospheric rupturing in form of fast propagating rift zones, and drastic changes of the spreading rate along the former spreading center, respectively, as mechanisms for transient excess melting by decompression. A combination of these inferred mechanisms and the Tristan da Cunha plume could satisfy the described observations from the South Atlantic.

Acknowledgements

We are very grateful to O. Eldholm and M. F. Coffin and two unnamed reviewers for critical review and helpful comments. Funding for this work was provided by the Bundesministerium für Bildung, Wissenschaft, Forschung und Technologie (BMBF), Deutsche For-

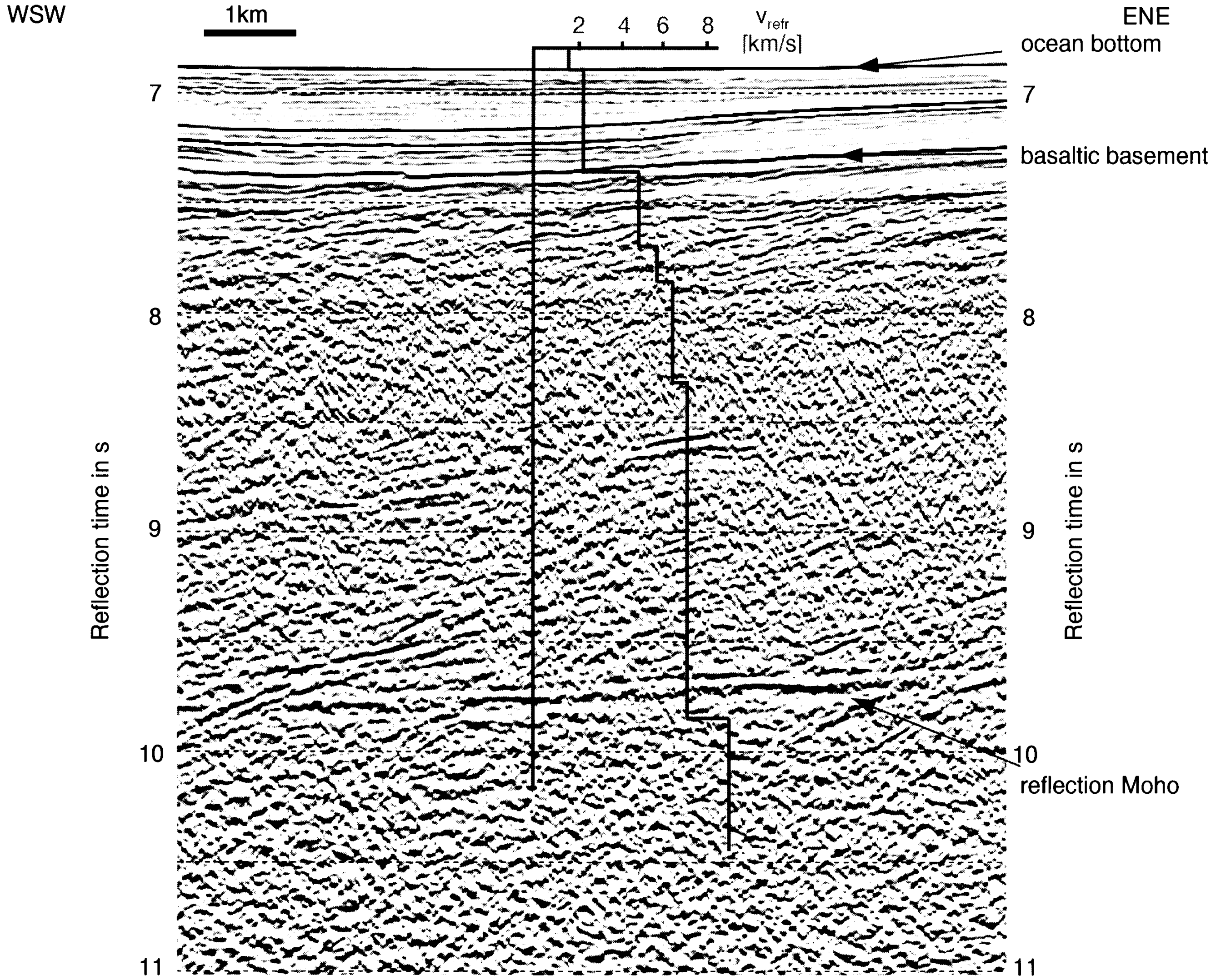

Fig. 23. Migrated seismic image of crustal category D showing the characteristic forms of reflectivity of this crustal category described in the text. The illustrated seismic section is also from the southern Angola Basin. The velocity-time function derived from results of wide-angle reflection/refraction measurements using ocean bottom hydrophone systems along the illustrated section is indicated.

schungsgemeinschaft (DFG), Bundesanstalt für Geowissenschaften und Rohstoffe (BGR).

References

Amaral, G., Cordani, U. G., Kawashita, K., & Reynolds, J. H. (1966). Potassium-argon dates of basaltic rocks from southern Brazil. *Geochim. Cosmochim. Acta*, *30*, 159–189.

Austin, J. A., & Uchupi, E. (1982). Continental-oceanic crustal transition off Southwest Africa. *AAPG Bull.*, *66*, 1328–1347.

Austin, J. A., Stoffa, P. L., Phillips, J. D., Oh, J., Sawyer, D. S., Prudy, G. M., Reiter, E., & Makris, J. (1990). Crustal structure of the southeast Georgia embayment—Carolina trough: Preliminary results of a composite seismic image of a continental suture (?) and a volcanic passive margin. *Geology*, *18*, 1023–1027.

Barron, J., Larsen, B. et al. (1991). *Proc. ODP*, *Sci. Results*, 119. College Station, TX: Ocean Drilling Program.

Bolli, H. M. et al. (1978). Cape Basin continental rise—Sites 360 and 361. *Init. Rep. of the Deep Sea Drilling Project*, *40*, 29–175.

Campbell, I. H., & Griffiths, R. W. (1990). Implications of mantle plume structure for the evolution of flood basalts. *Earth Planet. Sci. Lett.*, *99*, 79–93.

Cande, S., LaBrecque, J. L., Larson, R. L., Pitman III, N. C., Golovehenko, X., & Haxby, W. F. (1989). Magnetic Lineations of the world's ocean basins. *AAPG Map Series*, 1–14, Tulsa, Oklahoma.

Cannat, M. (1993). Emplacement of mantle rocks in the seafloor of mid-ocean ridges. *J. Geophys. Res.*, *98*, 4163–4172.

Christensen, N. I., & Smewing, J. A. (1981). Geology and seismic structure of the northern section of the Oman ophiolite. *J. Geophys. Res.*, *86*, 2545–2555.

Collins, J. A., Brocher, T. M., & Karson, J. A. (1986) Two-dimensional seismic reflection modelling of the inferred fossil oceanic crust/mantle transition in the Bay of Islands Ophiolite. *J. Geophys. Res.*, *91*, 12520–12538.

Cooper, A., Stagg, H., & Geist, E. (1991). Seismic stratigraphy and structure of Prydz Bay, Antarctica: Implications from Leg 119 drilling. In J, Barron & B. Larsen et al. (Eds.), *Proc. ODP*, *Sci. Results*, 119. College Station, TX: Ocean Drilling Program: 5.

Cordiani, U. G., Sartori, P. L. P., & Kawashita, K. (1980). Geoquimica dos isotopos de estronico e a evolucao da actividade vulcanica na Bacia do Paraná (sul do Brazil) durante o Cretocea. An. *Acad. Bras. Cienc.*, *52*, 811–818.

Duncan, R. A. (1984). Age progressive volcanism in the New England Seamounts and the opening of the Central Atlantic Ocean. *J. Geophys. Res.*, *89*, 9980–9990.

Duncan R. A., & Richards M. A. (1991). Hot spots, mantle plumes, flood basalts, and true polar wander. *Reviews of Geophysics*, *29*, 31–50.

Eldholm, O., Thiede, J., Taylor, E. et al. (1987). *Proc. ODP*, *Init. Rep.*, 104. College Station, TX: Ocean Drilling Program.

Eldholm, O., & Grue, K. (1994). North Atlantic volcanic margins: Dimensions and production rates. *J. Geophys. Res.*, *99*, 2955–2968.

Emery, K. O., Uchupi, E., Bowin, C. O., Phillips, J., & Simpson, E. S. W. (1975). Continental margin off western Africa: Cape St. Francis (South Africa) to Walvis Ridge (South-West Africa). *AAPG Bull.*, *59*, 3–59.

Ewing, M., Ludwig, W. J., & Ewing, J. (1964). Sediment distribution in the oceans: The Argentine Basin. *J. Geophys. Res.*, *69*, 2003–2017.

Ewing, J., & Lonardi, A. G. (1971). Sediment transport and distribution in the Argentine Basin, Part 5: Sedimentary structure of the Argentine Margin, Basin and related provinces. In L. H. Ahrens et al. (Eds.), *Physics and chemistry of the earth* Vol. 8, (pp. 123–251). Oxford: Pergamon Press.

Fitzgerald, M. G., Mitchum, R. M., Uliana, M. A., & Biddle, K. T. (1990). Evolution of the San Jorge Basin. *Argentin. Bull. AAPG*, *74*, 879–920.

Fritsch, J., Roeser, H. A., Bargeloh, H.-O., Block, M., Hinz, K., Kewitsch, P., Klein, A., and Schreckenberger, B. (1993). Variabilität der ozeanischen Kruste im Südatlantik VOKSA, FS Sonne-Fahrt SO85. *BGR-Report*, *111.103*, 1–120.

Gerrard, I., & Smith, G. C. (1983). The post Paleozoic succession and structure of the South-Western African continental margin. In J. S. Watkins & C. L. Drake (Eds.), *Studies in Continental Margin Geology*, Vol 34, (pp. 49–76). AAPG Mem.

Gladczenko, T. D., Hinz, K., Eldholm, O., Meyer, H., Neben, S., & Skogseid, J. (1997). South Atlantic volcanic margins. *J. Geol. Soc. London*, *154*, 465–470.

Goncalves de Souza, K. (1991). La marge sud-orientale brésilienne et les domoines oceaniques adjacents: structure et evolution. *Thèse de Doctorat de l'Université P. et M. Curie*—Paris *VI*, 230.

Hark, H.-U., & Hinz, K. (1995). Uruguay, In H. Kulke (Ed.), *Regional Petroleum Geology of the World. P. II* (pp. 577–581). Berlin–Stuttgart: Gebrüder Bornträger.

Hinz, K. (1981). A hypothesis on terrestrial catastrophies: wedges of very thick oceanward dipping layers beneath passive continental margins—their origin, and paleoenvironmental significance. *Geol. Jb.*, *E*23, 1–28.

Hinz, K., & Krause, W. (1982). The continental margin off Queen Maud Land/Antarctica: Seismic sequences, structural elements and geological development. *Geol. Jb.*, *E*23, 17–41.

Hinz, K., Mutter, J. C., Zehnder, C. M., and the NGT Study Group (1987). Symmetric conjugation of continent–ocean boundary along the Norwegian and East Greenland Margins. *Mar. Petrol. Geology*, *4*, 165–187.

Hinz, K., & BGR's Marine Geophysical Group (submitted). Distribution of Atlantic Volcanic Margins and Episodes of Intensive Production of Oceanic Crust in the Atlantic. submitted to *Marine Geophys. Researches*.

Hollister, C. D., Nowell, A. R. M., & Jumars, P. A. (1984). The dynamic abyss. *Scient. American*, *??*, 32–45.

Keeley, M. L., & Light, M. P. R. (1993). Basin evolution and prospectivity of the Argentine continental margin. *Journal Petroleum Geology*, *16*, 451–464.

Kempner, W. C., & Gettrust J. F. (1982a). Ophiolites, synthetic seismograms and oceanic crustal structure: 1. Comparison of ocean bottom seismometer data and synthetic seismograms for the Bay of Islands Ophiolite. *J. Geophys. Res.*, *87*, 8447–8462.

Kempner, W. C., & Gettrust, J. F. (1982b). Ophiolites, synthetic seismograms and oceanic crustal structure: 2. A comparison of synthetic seismograms of the Samail Ophiolite, Oman, and the ROSE refraction data from the East Pacific Rise. *J. Geophys. Res.*, *87*, 8462–8476.

Kennett, J. P., & Shackleton, N. J. (1976). Oxygen isotopic evidence for the development of the psychrosphere 38 Myr ago. *Nature*, *260*, 513–515.

Kennett, J. P., & Barker, P. F. (1990). Latest Cretaceous to Cenozoic climate and oceanographic developments in the Weddell Sea, Antarctica: An ocean-drilling perspective. *Proc. ODP*, *Sci. Res.*, 113, (pp. 937–960). College Station, TX: Ocean Drilling Program.

Kent, D. V., & Gradstein, F. M. (1986). A Jurassic to Recent chronology. In P. R. Vogt & B. E. Tucholke (Eds.), *The Geology of North Atlantic Region* Vol. M, (pp. 45–50). *The Western North Atlantic Region*.

LaBrecque, J. L., & Rabinowitz, P. D. (1977). Magnetic anomalies bordering the continental margin of Argentine. *AAPG Argentine Map Series*

Larsen, H. C., & Jakobsdottir, S. (1988). Distribution, crustal properties and significance of seaward-dipping sub-basement reflectors off E Greenland. In A. C. Morton & L. M. Parson (Eds.), *Early Tertiary Volcanism and the Opening of the NE Atlantic*. *Geol. Soc.*, *London Spec. Publ.*, *39*, 95–114.

Larsen, H. C., Saunders, A. D., Clift, P. D. et al. (1994). Proceedings of the Ocean Drilling Program, *Initial Reports*, 152. College, Station TX: Ocean Drilling Program.

Leg 152 Shipboard Party (1994). Drilling unearths 'Fire and Ice' at Southeast Greenland Margin. *EOS*, *Transactions*, *AGU*, *75*, 401–406.

Matthews, R., & Poore, R. Z. (1980). Tertiary ^{18}O record and glacio-eustatic sea-level fluctuations. *Geology*, *8*, 501–504.

Mutter, J. C., Talwani, M., & Stoffa, P. L. (1982). Origin of seaward-dipping reflectors in oceanic crust off the Norwegian margin by 'subaerial sea-floor spreading'. *Geology*, *10*, 353–357.

Mutter, J. C., Buck, W. R., & Zehnder, C. M. (1988). A model for the formation of thick basaltic sequences during the initiation of spreading. *J. Geophys. Res.*, *93*, 1031–1048.

Mutter, J. C., & Karson, J. A. (1992). Structural processes at slow-spreading ridges. *Science*, *257*, 627–634.

Nicolas, A. (1989). The various ophiolites and their oceanic environments of origin. In A. Nicolas (Ed.), *Structures of ophiolites and dynamics of oceanic Lithosphere*. London: Kluwer Academic Publishers.

Nürnberg, D., & Müller, R. D. (1991). The tectonic evolution of the South Atlantic from Late Jurassic to present. *Tectonophysics*, *191*, 27–53.

Parsons, B., & Sclater, J. G. (1977). An analysis of the variation of ocean floor bathymetry and heat flow with Age. *J. Geophys. Res.*, *82*, 803–827.

Rabinowitz, P. D., & LaBrecque, J. (1979). The Mesozoic South Atlantic Ocean and evolution of its continental margins. *J. Geophys. Res.*, *84*, 5973–6002.

Ramos, V. A., & Turic, M. A. (1996). Geologia y recursos naturales de la plataforma continental Argentina. Buenos Aires, 452.

Renkin, M. L., & Sclater, J. G. (1988). Depth and age in the North Pacific. *J. Geophys. Res.*, *93*, 2919–2936.

Renne, P. R., Mertz, D. F., Teixeiva, W., Ens, H. H., & Richards, M. A. (1993). Geochronologic Constraints on Magmatic and Tectonic Evolution of the Paraná Province. *Eos*, *Transactions*, *AGU*, *43*, 553.

Richards, M. A., Duncan, R. A., & Courtillot, V. E. (1989). Flood basalts and hotspot tracks: Plume heads and tails. *Science*, 246, 103–107.

Roberts, D. G., Backman, J., Morton, A. C., Murray, J. W., & Keene, J. B. (1984). Evolution of volcanic rifted margins: Synthesis of Leg 81 results on the west margin of Rockall Plateau. In D. G. Roberts & D. Schnittker (Eds.), *Init. Rep. of the Deep Sea Drilling Project* Vol. 81, (pp. 883–991). Washington: U.S. Government Printing Office.

Roberts, D. G., Schnitker, D. et al. (1984). Initial Reports of the Deep Sea Drilling Project, Leg 81, Washington: U.S. Government Printing Office, *81*.

Sartori, P. L., Maciel Filho, C., & Menegott, E. (1975). Contribution of the study of Paraná Basin volcanic rocks in the region of Santa Maria, State of Rio Grande do Sul. *Rev. Bras.*, *Geosciencias*, *5*, 141–159.

Schönharting, G., & Abrahamsen, N. (1989). Paleomagnetism of the volcanic sequences in hole 642E, ODP Leg 104, Voring Plateau, and correlation with early Tertiary basalts in the North Atlantic. In O. Eldholm, J. Thiede, E. Taylor et al. (Eds.), *Proc. ODP*, *Sci. Results*, 104, College Station, TX: Ocean Drilling Program.

Schreckenberger B. (1997). Magnetische Anomalien über seewärts einfallenden seismischen Reflektorfolgen—eine vergleichende Untersuchung verschiedener Vorkommen im Atlantik. Ph. D. thesis, Frankfurt University, Germany.

Sibuet, J.-C., Hay, W. W., Prunier, A., Montadert, L., Hinz, K., Fritsch, J. (1984). Early evolution of the South Atlantic Ocean: Role of the rifting episode. *Initial Reports of the Deep Sea Drilling Projekt*, Vol. 75, (pp. 469–481). Washington: U.S. Government Printing Office.

Skogseid, J., & Eldholm, O. (1987). Early Cenozoic crust at the Norwegian continental margin and the conjugate Jan Mayen Ridge. *J. Geoph. Res.*, *91*, 11471–11491.

Smythe,, D. K. (1983). Faeroe–Shetland escarpment and continental margin north of the Faeroes. In M. H. P. Bott, S. Saxov, M. Talwani and J. Thiede (Eds.), *Structure and development of the Greenland–Scotland ridge* (pp. 109–119). New York: Plenum Press.

Supko, P. R., & Perch-Nielsen, K. (1977). General synthesis of Central and South Atlantic Drilling Results, Deep Sea Drilling Project. *Init. Rep. of the Deep Sea Drilling Project* Vol. 39, (pp. 1099–1132). Washington: U.S. Government Printing Office.

Stoakes, F. A., Campbell, C. V., Cass, R., & Ucha, N. (1991). Seismic stratigraphic analysis of the Punta del Este basin, offshore Uruguay. *South America*. *Bull. AAPG*, *75*, 219–240.

Thorarinsson, S., 1968. Some problems of volcanism in Iceland. *Geol. Rundschau*, *57*, 1–20.

Uliana, M. A., Biddle, K. T., & Cerdan, J. (1989). Mesozoic extension and formation of Argentine sedimentary basins. In A. J. Tankard and H. R. Balkwill (Eds.) *Extensional tectonics and stratigraphy of the North Atlantic margins* Vol. 46 (pp. 599–614). AAPG Mem.

Van Der Voo, R. (1993). *Paleomagnetism of the Atlantic*, *Thetys and Iapetus ocean*. Cambridge University Press.

White, R. S., Spence, G. D., Fowler, S. R., McKenzie, D. P., Westbrook, G. K., & Bowen, A. N. (1987). Magmatism at rifted continental margins. *Nature*, *330*, 439–444.

White, R. S., & McKenzie, D. P. (1989). Magmatism at rift zones: The generation of volcanic continental margins and flood basalts. *J. Geophys. Res.*, *94*, 7685–7730.